PHYSICAL REVIEW A VOLUME 28, NUMBER 2 AUGUST 1983

Landau theory of cholesteric blue phases

H. Grebel, R. M. Hornreich, and S. Shtrikman
Department of Electronics, Weizmann Institute of Science, Rehovot 76100, Israel

(Received 30 June 1982)

A detailed presentation of the Landau theory of the cholesteric blue phase (BP) is given with emphasis on the comparison of model predictions with reported experimental data. The basic model, which is asymptotically exact in the high-chirality limit, leads to the prediction of a body-centered cubic (bcc) O^5 ($I432$) structure for the BP. However, the model can be systematically extended to physical chiralities and used to calculate the free energies of more complex cubic structures. In particular, bcc O^8 ($I4_132$) and simple-cubic O^2 ($P4_232$) structures are analyzed and their optical and thermodynamic properties, as well as those of O^5, are compared with those reported for the two observed phases, BPI and BPII. It is shown that, in general, the known properties of these phases are consistent with a structure assignment of O^8 for BPI and O^2 for BPII. Some promising lines for future investigation are indicated.

I. INTRODUCTION

The nature and properties of the anomolous phases which appear in many cholesteric liquid-crystal systems below their clearing point, and which are known collectively as the "blue phase" (BP), are being intensively investigated both experimentally[1-11] and theoretically.[12-17] The experimental situation can be briefly summarized as follows.

(1) The anomalous phases appear only for cholesteric systems having a "short" pitch in the usual cholesteric (helicoidal) phase.[1,3,5,7,10] That is, if the cholesteric pitch is increased by, e.g., mixing the cholestegen with a nematic system, the BP region will narrow and, eventually, vanish as shown schematically in Fig. 1.

(2) The BP region is relatively narrow (1—2 K).[1-11]

(3) The BP region appears to consist of at least three subregions,[1-11] which have been labeled, as shown in Fig. 1, BPI, BPII, and BPIII. (The latter has also been referred to as the "gray" or "fog" phase.)

(4) BPI and BPII, while thermodynamically distinct phases,[1] have very similar optically properties. In particular, they are nonbirefringent, optically active, and exhibit several sharp Bragg peaks. The latter, for both BPI and BPII, are consistent with both body-centered and simple cubic structures.[2,3,7,11]

(5) BPIII does not exhibit Bragg peaks but its light-scattering properties are, e.g., strongly sensitive to the sense of circularly polarized incident light.[2] It has been suggested[2] that BPIII is a thermodynamically distinct phase but the evidence for this point of view is still not compelling.

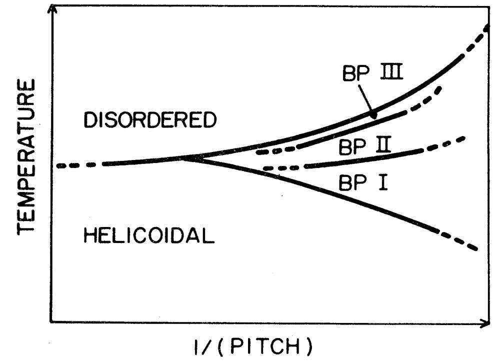

FIG. 1. Schematic phase diagram, showing the three experimental observed blue phases (BP).

Theoretically, using Landau theory,[18,19] we have shown[12(a)-12(e)] that there can indeed exist thermodynamically stable cubic phases in a narrow temperature region between the disordered (isotropic) and ordinary cholesteric phases when the cholesteric pitch is sufficiently short. Since the experimental evidence to date strongly supports the viewpoint that BPI and BPII have cubic structures, we believe that a detailed and unified presentation of the Landau theory of cholesterics will be useful to all workers in the field. This is particularly necessary as the notations and presentation of the results of the various Landau calculations[12,13,16,20] differ greatly from each other, making comparison with experiment difficult. We shall particularly emphasize those results of our model calculations which can be compared with the existing experimental data. In addition, we shall show how the basic Landau theory can be naturally extended to include more complex cubic structures.

The organization of this paper is as follows. In Sec. II we present the basic Landau theory of phase transitions in cholesterics and analyze the transition from the isotropic (I) to the usual helicoidal (C) phase. We then consider the high-chirality (short-pitch) limit and show that a transition from I to a body-centered cubic phase with O^5 ($I432$) symmetry will occur. The thermodynamic properties of the C and O^5 phases are given. Finally, we consider briefly the planar hexagonal structure suggested originally by Brazovskii and Dmitriev[20] and show that this phase is not expected to be thermodynamically stable.

In Sec. III we consider in detail the role played by harmonics of the basic order parameter. After presenting selection rules for the structure factor in cubic liquid crystal phases, we calculate Landau free energies for body-centered cubic O^8 ($I4_132$) and simple-cubic O^2 ($P4_232$) structures. We find that these phases will be stable in certain regions of the phase diagram shown in Fig. 1. The thermodynamic properties of the O^8 and O^2 phases are considered. Finally, in Sec. IV, we compare our calculated results with the available experimental data and indicate lines for future work.

II. BASIC LANDAU THEORY OF PHASE TRANSITIONS IN CHOLESTERICS

A. General considerations

The Landau theory of phase transitions[18] is based upon choosing an order parameter which vanishes in the high-symmetry phase and becomes nonzero when the system undergoes a transition to a lower-symmetry phase. For the case of isotropic-to-nematic (I-to-N) or isotropic-to-cholesteric (I-to-C) phase transitions in thermotropic liquid crystals, an appropriate choice is the anisotropic part of the dielectric tensor

$$\epsilon_{ij}(\vec{r})=\epsilon_{ij}^{d}(\vec{r})-\tfrac{1}{3}\mathrm{Tr}(\epsilon^{d})\delta_{ij}\ .$$

For cholesteric systems, the average free-energy density is then given by[19,20]

$$F=V^{-1}\int d\vec{r}\{\tfrac{1}{2}[a\epsilon_{ij}^{2}+c_{1}\epsilon_{ij,l}^{2}+c_{2}\epsilon_{ij,i}\epsilon_{lj,l}-2de_{ijl}\epsilon_{in}\epsilon_{jn,l}]-\beta\epsilon_{ij}\epsilon_{jl}\epsilon_{li}+\gamma(\epsilon_{ij}^{2})^{2}\}\ , \tag{1}$$

where, as usual, a is proportional to a reduced temperature, c_1, c_2, d, β, and γ are regarded as temperature-independent parameters,

$$\epsilon_{ij,l}\equiv\partial\epsilon_{ij}/\partial x_{l}\ ,$$

and we sum on repeated indices. For thermodynamic stability, it is clear that c_1 and γ must be positive. Restrictions on c_2 will be given below. Note that (1) contains *all* symmetry-allowed invariants up to fourth order in ϵ_{ij} and includes for the quadratic part, those involving first-order spatial derivatives of ϵ_{ij} as well. Higher order contributions, which could be significant,[12(f)] will not be considered here. There is only one fourth-order invariant in (1) since

$$(\epsilon_{ij}^{2})^{2}=2\epsilon_{ij}\epsilon_{jl}\epsilon_{ln}\epsilon_{ni}\ .$$

Without loss of generality, we shall henceforth assume that $d>0$.

Since we shall be interested in periodic structures, it will be convenient to expand $\epsilon_{ij}(\vec{r})$ in Fourier components

$$\epsilon_{ij}(\vec{r})=\sum_{h,k,l}N^{-1/2}\epsilon_{ij}(\sigma)\exp[iq(hx+ky+lz)]\ , \tag{2a}$$

where $\sigma=h^2+k^2+l^2$, $N=(3!)2^{3-n_0}/(n_1!)$, where n_0 (n_1) is the number of vanishing (equal) $|h|,|k|,|l|$, and, for *each* $[h,k,l]$ (including $h=k=l=0$),

$$\begin{aligned}[\epsilon(\sigma)]&=\sum_{m=-2}^{2}\epsilon_{m}(\sigma)e^{i\psi_{m}(h,k,l)}[M_{m}(h,k,l)]\\&=\tfrac{1}{2}\left[\epsilon_{2}e^{i\psi_{2}}\begin{bmatrix}1&i&0\\i&-1&0\\0&0&0\end{bmatrix}+\epsilon_{1}e^{i\psi_{1}}\begin{bmatrix}0&0&1\\0&0&i\\1&i&0\end{bmatrix}+\sqrt{2/3}\,\epsilon_{0}e^{i\psi_{0}}\begin{bmatrix}-1&0&0\\0&-1&0\\0&0&2\end{bmatrix}\right.\\&\qquad\left.+\epsilon_{-1}e^{i\psi_{-1}}\begin{bmatrix}0&0&-1\\0&0&i\\-1&i&0\end{bmatrix}+\epsilon_{-2}e^{i\psi_{-2}}\begin{bmatrix}1&-i&0\\-i&-1&0\\0&0&0\end{bmatrix}\right]\end{aligned} \tag{2b}$$

with $\epsilon_m(\sigma)\geq 0$ and $\psi_m(h,k,l)=-\psi_m(-h,-k,-l)$. Note that the basis matricies $[M_m]$ are such that $[h,k,l]$ is along the polar axis of a local coordinate system which is defined separately for each $[h,k,l]$.

Since the $[M_m]$ matrices in (2b) are equivalent to the five $j=2$ spherical harmonics, an alternate form for the order parameter is

$$\Phi(\vec{r})=\sum_{h,k,l;m} N^{-1/2}\epsilon_m(\sigma)\{Y_2^m(h,k,l)\exp[iq(hx+ky+lz)+i\psi_m(h,k,l)]\}\ , \tag{3}$$

where $Y_j^m(h,k,l)$ is the (j,m) spherical harmonic in the chosen local coordinate system whose polar axis is along $[h,k,l]$. Although we used this representation in our earlier work,[12(a)–12(e)] we shall here use the tensor form (2) and calculate F using (1).

The calculation of the quadratic part of F is straightforward and the resulting expression is

$$\begin{aligned}F_2&=\tfrac{1}{2}\sum_{h,k,l;m} N^{-1}\{a-mdq(h^2+k^2+l^2)^{1/2}+[c_1+\tfrac{1}{6}c_2(4-m^2)]q^2(h^2+k^2+l^2)\}\epsilon_m^2(\sigma)\\&=\tfrac{1}{2}\sum_{\sigma,m}\{a-mdq\sigma^{1/2}+[c_1+\tfrac{1}{6}c_2(4-m^2)]q^2\sigma\}\epsilon_m^2(\sigma)\ .\end{aligned} \tag{4}$$

For thermodynamic stability we must require, in addition to $c_1>0$, that $c_1+\frac{2}{3}c_2>0$.

Since, in Landau theory, the explicit q dependence of higher than second-order contributions to F is ignored, we have $\partial F/\partial q=\partial F_2/\partial q=0$ and, from (4), we obtain

$$\begin{aligned}r\equiv\frac{q}{q_0}&=\left[\sum_{h,k,l;m} N^{-1}[m(h^2+k^2+l^2)^{1/2}\epsilon_m^2(\sigma)]\right]\Bigg/\left[\sqrt{2}\sum_{h,k,l;m}\{N^{-1}[1+\tfrac{1}{6}(4-m^2)(c_2/c_1)]\right.\\&\qquad\left.\times(h^2+k^2+l^2)\epsilon_m^2(\sigma)\}\right]\\&=\left[\sum_{\sigma;m}[m\sigma^{1/2}\epsilon_m^2(\sigma)]\right]\Bigg/\left[\sqrt{2}\sum_{\sigma;m}\{[1+\tfrac{1}{6}(4-m^2)(c_2/c_1)]\sigma\epsilon_m^2(\sigma)\}\right]\ ,\end{aligned} \tag{5}$$

with $q_0\equiv d/\sqrt{2}c_1$. The $h=k=l=\sigma=0$ term is excluded from the sums in (5).

For nonchiral (nematic or racemic) systems, $d=0$, and the transition from the isotropic state is to a phase with $q=0$. The excitation spectrum $F_2(q)$ for such a system is illustrated in Fig. 2(a). When $d\neq0$, the system is chiral or cholesteric and the minimum in the excitation spectrum is no longer at $q=0$, as shown in Fig. 2(b). Note that the ther-

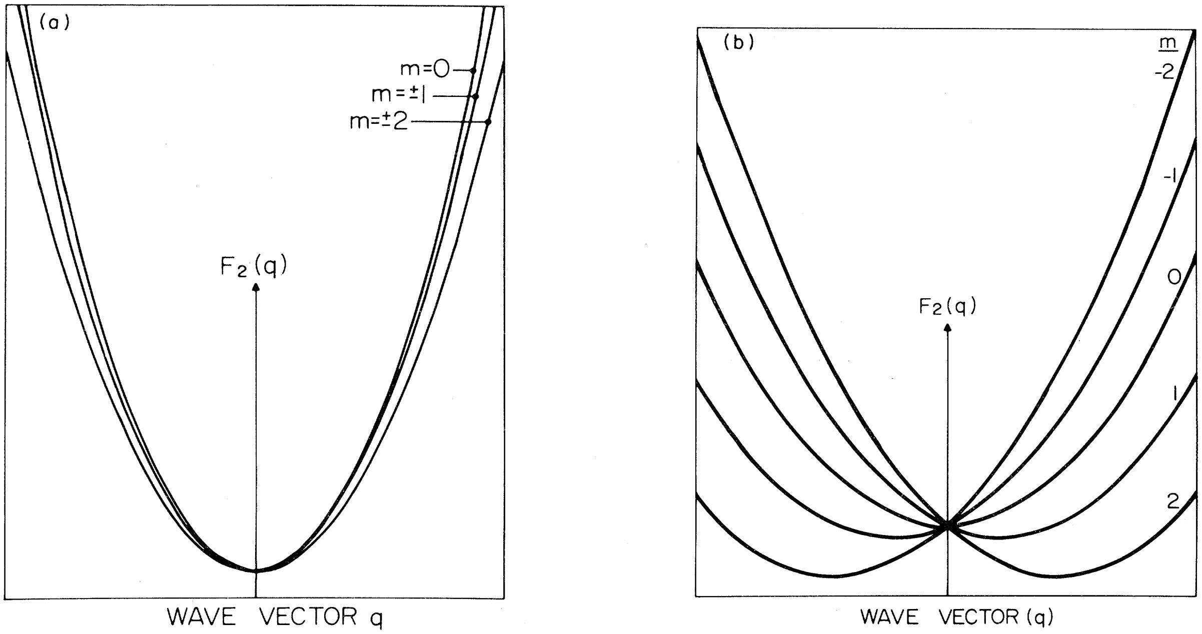

FIG. 2. Wave vector (q) and eigenvalue (m) dependence of the quadratic part of the Landau free energy for (a) a nematic liquid crystal or a racemic mixture, (b) a cholesteric liquid crystal.

modynamic stability condition $c_1+\frac{2}{3}c_2>0$ guarantees that the ground state will *always* belong to the $m=2$ branch (for $d>0$) of the excitation spectrum. (The claim by Brazovskii and co-workers[20] that for $c_2<0$ the ground state would belong to the $m=1$ branch was due to an algebraic error and is incorrect.)

B. Helicoidal phase

The usual helicoidal cholesteric (C) phase is characterized by a single nonzero wave vector and, as noted above, will necessarily be a transverse ($m=2$ for $d>0$) spiral. From (5), the equilibrium value of the C phase wave vector is

$$q_C \equiv q_0(h^2+k^2+l^2)^{1/2} = \sqrt{2}q_0 = d/c_1 \ , \tag{6}$$

and the Bragg backreflection wavelength (in the material) is

$$\lambda_C = 4\pi/q_C = 4\pi/\sqrt{2}q_0 \ .$$

Aside from the $\pm q_C$ Fourier components, the description of the *I*-*C* phase transition requires an additional $q=0$ order-parameter component, associated with the $m=0$ branch of the excitation spectrum. This is shown schematically in Fig. 3(a). The tensor order parameter ϵ^C thus takes the *exact* form

$$[\epsilon^C(\vec{r})] = \frac{-1}{\sqrt{6}}\epsilon_0(0)\begin{bmatrix} -1 & 0 & 0 \\ 0 & -1 & 0 \\ 0 & 0 & 2 \end{bmatrix} + \frac{1}{2\sqrt{2}}\epsilon_2(2)\left[\exp\{i[q_c z+\psi_2(2)]\}\begin{bmatrix} 1 & i & 0 \\ i & -1 & 0 \\ 0 & 0 & 0 \end{bmatrix} + \text{c.c.} \right] , \tag{7}$$

where c.c. denotes complex conjugate. Upon substituting into (1), using (4)–(6), and noting that $(M_m)_{ij}(M_{m'})_{ji}=\delta_{m(-m')}$, we obtain

$$F_C = \tfrac{1}{2}[a\epsilon_0^2(0)+(a-d^2/c_1)\epsilon_2^2(2)] - \frac{1}{\sqrt{6}}\beta[\epsilon_0^3(0)-3\epsilon(0)\epsilon_2^2(2)]+\gamma[\epsilon_0^2(0)+\epsilon_2^2(2)]^2 \ . \tag{8}$$

Equation (8) can be put into a more convenient form by introducing the reduced quantities:

$$\epsilon = s\mu, \quad s=\beta/\sqrt{6}\gamma, \quad f=F/(\beta^4/36\gamma^3) \ ,$$
$$\tfrac{1}{4}t=(3\gamma/\beta^2)a, \quad \tfrac{1}{4}\xi_R^2=(3\gamma/\beta^2)c_1, \quad \kappa=q_C\xi_R \ . \tag{9}$$

Substituting (9) into (8) gives

$$f_C=\tfrac{1}{4}t\mu_0^2(0)+\tfrac{1}{4}(t-\kappa^2)\mu_2^2(2)+[\mu_0^3(0)-3\mu_0(0)\mu_2^2(2)]+[\mu_0^2(0)+u_2^2(2)]^2 \ . \tag{10}$$

The meaning of the reduced temperature t and correlation length ξ_R can now be understood by considering a racemic (R) mixture, where $q_C=\kappa=0$. It is easily verified that $f_R=f_C(\kappa=0)$ is minimized when $\mu_2(2)/\mu_0(0)=\sqrt{3}$. Defining

$$\mu^2=\mu_0^2(0)+\mu_2^2(2) \ ,$$

we then have

$$f_R=\tfrac{1}{4}t\mu^2-\mu^3+\mu^4 \ . \tag{11}$$

Setting $f_R=\partial f_R/\partial\mu=0$, we find that the isotropic-racemic (*I*-*R*) thermodynamic phase boundary is at $t=t_R=1$. From (9), it follows that ξ_R is simply the correlation length for a racemic mixture on the *I*-*R* phase boundary and that the reduced temperature unit is the difference between the thermodynamic and extrapolated-from-the-disordered phase transition temperatures for a racemic mixture.

We now return to the general case $\kappa\neq 0$. A convenient way of determining the *I*-*C* transition temperature t_{IC} is to use variables μ,θ, which are related to $\mu_0(0),\mu_2(2)$ by $\mu_0(0)=\mu\sin\theta$, $\mu_2(2)=\mu\cos\theta$, and to set $f_C=\partial f_C/\partial\mu=\partial f_C/\partial\theta=0$. From (10), we obtain, in addition to the solution $\mu=0$, the equation

$$\tfrac{1}{4}t_{IC}-\tfrac{1}{4}\kappa^2\cos^2\theta+(\sin^3\theta-3\sin\theta\cos^2\theta)\mu+\mu^2=0 \ , \tag{12a}$$

$$\tfrac{1}{2}t_{IC}-\tfrac{1}{2}\kappa^2\cos^2\theta+3(\sin^3\theta-3\sin\theta\cos^2\theta)\mu+4\mu^2=0 \ , \tag{12b}$$

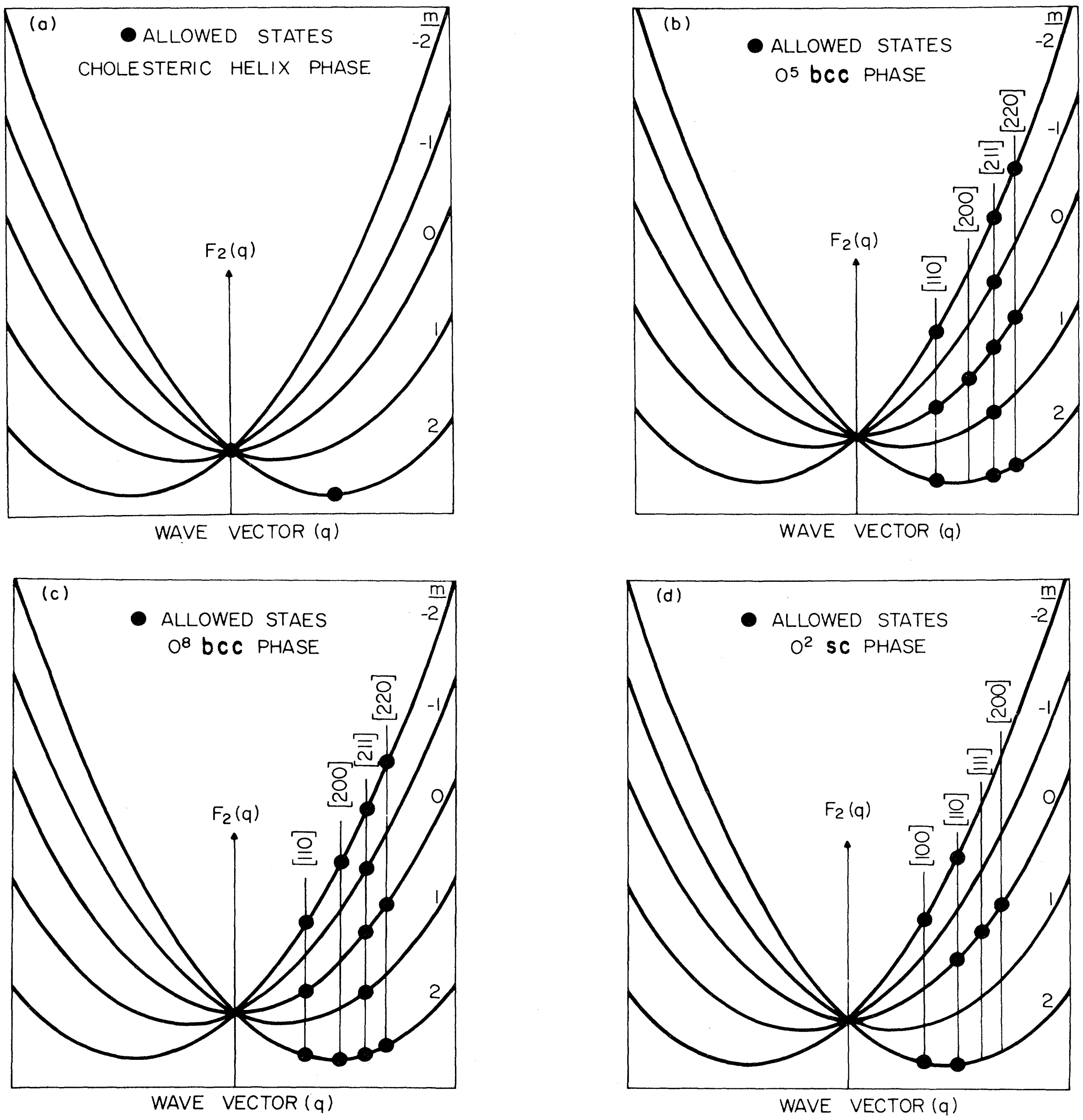

FIG. 3. Wave vector (q) and eigenvalue (m) dependence of the quadratic part of the Landau free energy, showing allowed states for (a) the cholesteric helicoidal structure, (b) the bcc O^5 ($I432$) structure, (c) the bcc O^8 ($I4_132$) structure, (d) the sc O^2 ($P4_232$) structure.

$$\tfrac{1}{2}\kappa^2\sin\theta+3(4\sin^2\theta-1)\mu=0\ . \tag{12c}$$

Combining (12a) and (12b) gives

$$\mu=-\tfrac{1}{2}(\sin^3\theta-3\sin\theta\cos^2\theta)\ . \tag{13a}$$

Substituting (13a) into (12c), we solve for θ, obtaining

$$4\sin^2\theta=2-(1+\tfrac{1}{3}\kappa^2)^{1/2}\ . \tag{13b}$$

From (13a) and (13b) we see that for $\kappa>3$ only the alternate solution, $\mu=0$, is allowed. In other works, *for sufficiently short pitch, $q_C\geq 3/\xi_R$, the I-C phase transition, if it exists, must be of second order and will occur at $t=t_{IC}=\kappa^2$.*

For $q\leq 3/\xi_R$, t_{IC} can be obtained by substituting (13a) and (13b) into the following combination of (12a) and (12b):

$$\tfrac{1}{2}t_{IC}-\tfrac{1}{2}\kappa^2\cos^2\theta+(\sin^3\theta-3\sin\theta\cos^2\theta)\mu=0\ . \tag{12d}$$

We have finally

$$t_{IC}=\begin{cases}\tfrac{1}{2}[1+\kappa^2+(1+\tfrac{1}{3}\kappa^2)^{3/2}], & \text{for } \kappa\le 3\\ \kappa^2, & \text{for } \kappa>3\ .\end{cases} \tag{13c}$$

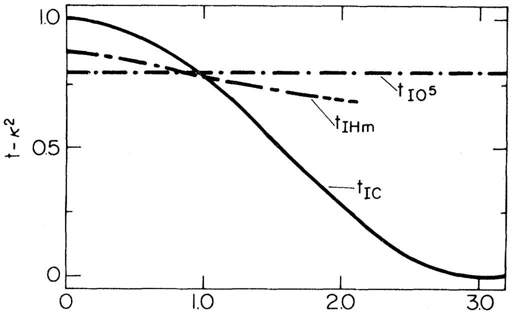

FIG. 4. Theoretical phase diagram showing the thermodynamic boundaries between the isotropic (I) and cholesteric helicoidal (C) phases (t_{IC}), the I and bcc O^5 phases (t_{IO^5}), and the I and hexagonal (Hm) phases (t_{IHm}), as a function of chirality parameter κ.

This phase boundary is shown graphically in Fig. 4.

Also of interest are the change of entropy associated with the I-C phase transition and the asymmetry parameter, which measures the local biaxiality of the ordered phase. From (10) we have for the former

$$\Delta S_{IC}\equiv 16df_C/dt\,|_{t=t_{IC}}=\begin{cases}4\mu^2(t_{IC})=\tfrac{1}{4}[2+3(1+\tfrac{1}{3}\kappa^2)^{1/2}-(1+\tfrac{1}{3}\kappa^2)^{3/2}], & \kappa\le 3\\ 0, & \kappa>3\ .\end{cases} \tag{14}$$

Note that we have normalized ΔS so that $\Delta S_{IC}(\kappa=0)\equiv\Delta S_R=1$. $\Delta S_{IC}(\kappa)$ is shown graphically in Fig. 5.

The asymmetry parametry $\eta(\vec{r})$ $(0\le\eta\le 1)$ is determined by diagonalizing $[\epsilon(\vec{r})]$ for given $\vec{r}$ and rewriting the resulting matrix in the form

$$[\epsilon]\equiv\epsilon\begin{bmatrix}\tfrac{1}{2}(-1-\eta) & 0 & 0\\ 0 & \tfrac{1}{2}(-1+\eta) & 0\\ 0 & 0 & 1\end{bmatrix}\ . \tag{15a}$$

In the C phase, $\eta=\eta_C$ is independent of $\vec{r}$ and, from (7), we have at $t=t_{IC}$

$$\eta_C=1-2\tan\theta/(\sqrt{3}-\tan\theta)\ , \tag{15b}$$

with θ given by (13b).

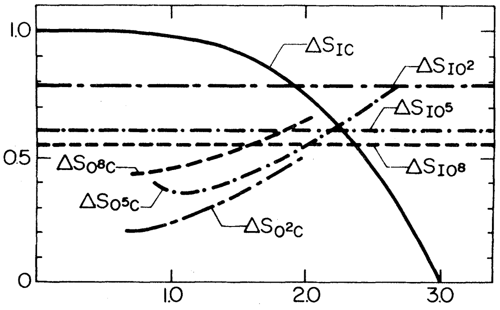

FIG. 5. Entropy changes ΔS associated with the different phase transitions as a function of chirality parameter κ.

C. High-chirality limit: The bcc O^5 phase

In Sec. II B we showed that for $\kappa\ge 3$ the I-C phase transition would necessarily be of second order. There immediately arises the question of whether a *first-order* transition, from the isotropic to some other ordered phase, is possible. Such a transition, which would, of course, occur at $t>t_{IC}$, *necessarily results in a structure whose free energy, in some region of temperature and pitch, is lower than that of either the I or C phases.* It could, therefore, be thermodynamically stable. Since a global minimization of (1) for arbitrary κ is extremely difficult (see Appendix), it is useful to first consider the *high-chirality region,* $\kappa\gg 1$.

When $\kappa\to\infty$, it is clear from (4) and Fig. 2(b) that any structure which minimizes the free energy will have only $m=2$ Fourier components associated with wave vectors of magnitude

$$q_0(h^2+k^2+l^2)^{1/2}=\sqrt{2}q_0=q_C\ .$$

In addition, since we are interested in a first-order phase transition, it is clear that there must exist a nonzero third-order contribution to F. This is possible only if the wave vectors associated with the Fourier components of ϵ_{ij} form one or more equilateral triangles.[21,22] The simplest possible three-dimensional structure, a regular tetrahedron of wave vectors, is illustrated in Fig. 6.

We choose our spatial axes such that the wave vectors in Fig. 6 lie along $\langle 110\rangle$ directions. Clearly, they generate an fcc structure in the reciprocal space. The labeling of the wave vectors is given in Table I. The order parameter takes the form

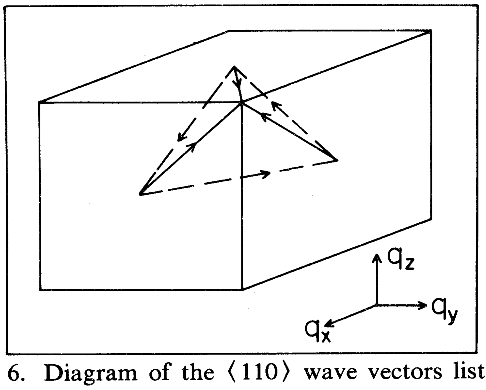

FIG. 6. Diagram of the ⟨110⟩ wave vectors listed in Table I, illustrating how they generate a face-centered cubic lattice in reciprocal space.

TABLE I. Wave vectors and local axis systems $(\hat\xi,\hat\eta,\hat\zeta)$ for the ⟨110⟩ wave vectors illustrated in Fig. 6. For the wave vectors $-\vec{q}_{2n}$, $\hat\eta_{2n}$ is replaced by $-\hat\eta_{2n}$. The wave vector q is determined, in general, from (5).

Wave vector $(\vec{q}_{2n}=\sqrt{2}q\hat\zeta_{2n})$	$\hat\xi_{2n}$	$\hat\eta_{2n}$
$\vec{q}_{21}=\sqrt{2}q[(\hat{x}+\hat{y})/\sqrt{2}]$	$\hat{z}$	$(\hat{x}-\hat{y})/\sqrt{2}$
$\vec{q}_{22}=\sqrt{2}q[(\hat{y}+\hat{z})/\sqrt{2}]$	$\hat{x}$	$(\hat{y}-\hat{z})/\sqrt{2}$
$\vec{q}_{23}=\sqrt{2}q[(\hat{z}+\hat{x})/\sqrt{2}]$	$\hat{y}$	$(\hat{z}-\hat{x})/\sqrt{2}$
$\vec{q}_{24}=\sqrt{2}q[(-\hat{x}+\hat{y})/\sqrt{2}]$	$-\hat{z}$	$-(\hat{x}+\hat{y})/\sqrt{2}$
$\vec{q}_{25}=\sqrt{2}q[(-\hat{y}+\hat{z})/\sqrt{2}]$	$-\hat{x}$	$-(\hat{y}+\hat{z})/\sqrt{2}$
$\vec{q}_{26}=\sqrt{2}q[(-\hat{z}+\hat{x})/\sqrt{2}]$	$-\hat{y}$	$-(\hat{z}+\hat{x})/\sqrt{2}$

$$[\epsilon^B(\vec{r})]=(\tfrac{1}{12})^{1/2}\sum_{n=1}^{6}\epsilon_2(2)([M_2(2n)]\exp\{i[\vec{q}_{2n}\cdot\vec{r}+\psi_2(2n)]\}+\text{c.c.})\ , \qquad (16)$$

where both the tensor

$$[M_m(\sigma n)]=[M_2(2n)]=\tfrac{1}{2}\begin{bmatrix}1 & i & 0\\ i & -1 & 0\\ 0 & 0 & 0\end{bmatrix}\ ,$$

and the phase $\psi_m(\sigma n)=\psi_2(2n)$, are *defined in the local axis system associated with the wave vector* $\vec{q}_{\sigma n}=\vec{q}_{2n}$ (see Table I).

The quadratic part of the free energy F_B is found from (4) and (5) and is simply

$$(F_2)_B=\tfrac{1}{2}(a-d^2/c_1)\epsilon_2^2(2)\ . \qquad (17)$$

To evaluate the cubic and quartic parts of the free energy it is necessary to express the $[M_2(2n)]$ in a common coordinate system. This can be done in several ways. A convenient approach is to use a dyadic notation for the elements of the basis tensors $[M_2(\sigma n)]$. Following Brazovskii and co-workers[20] we write

$$[M_2(\sigma n)]_{\alpha\beta}=u_\alpha(\sigma n)u_\beta(\sigma n)\ , \qquad (18a)$$

with

$$\hat{u}\equiv(\hat\xi+i\hat\eta)/\sqrt{2}\ . \qquad (18b)$$

Here $\hat\xi,\hat\eta$ are real unit vectors, taken such that $\hat\xi$, $\hat\eta$, and

$$\hat\zeta\equiv(h\hat{x}+k\hat{y}+l\hat{z})/(h^2+k^2+l^2)^{1/2}$$

form a local right-handed coordinate system. For the wave vectors shown in Fig. 6 the corresponding local axis systems are given in Table I. Note that in the complex conjugate segment of the order parameter, where $\vec{q}_{2n}\rightarrow-\vec{q}_{2n}$, we replace $\hat\eta_{2n}$ by $-\hat\eta_{2n}$ so as to preserve the right handedness of the local axis systems. The scalar products relevant to the calculation of the cubic and quartic invariants are summarized in Table II.

The cubic part of the free energy is obtained by considering all closed triangles of wave vectors [see Fig. 7(a)]. By inspection of Fig. 6, we have

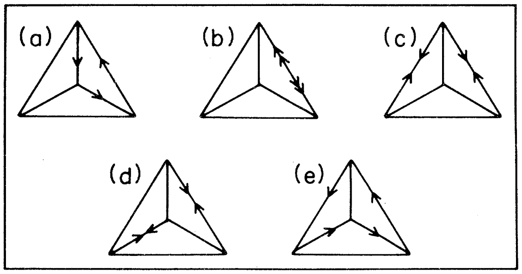

FIG. 7. Diagrammatic contributions to the free energy of the bcc O^5 phase (a) the cubic contribution, (b)—(e) quartic contributions.

TABLE II. Scalar products for the complex basis vectors $\hat{u}(2n)\equiv[\hat\xi(2n)]+i\hat\eta(2n)]/\sqrt{2}$ $(n=1,\ldots,6)$. All other products can be found by cyclic permutation and complex conjugation.

	$\hat{u}(21)$	$\hat{u}(22)$	$\hat{u}(24)$	$\hat{u}(25)$	$\hat{u}(26)$
$\hat{u}(21)$	0	$\frac{1}{4}$	$-\frac{1}{2}$	$\frac{3}{4}e^{-i\alpha_0}$	$\frac{1}{4}$
$\hat{u}(24)$			0	$\frac{3}{4}e^{i\alpha_0}$	
$\hat{u}^*(21)$	1	$\frac{3}{4}e^{-i\alpha_0}$	$-\frac{1}{2}$	$\frac{1}{4}$	$\frac{3}{4}e^{-i\alpha_0}$
$\hat{u}^*(24)$			1	$\frac{1}{4}$	

$$
\begin{aligned}
(F_3)_B = -3!(\tfrac{1}{12})^{3/2}\beta\epsilon_2^3(2)(&\operatorname{Tr}[M_2(21)M_2^*(22)M_2^*(26)] \\
&\times\exp\{i[\psi_2(21)-\psi_2(22)-\psi_2(26)]\}+\text{c.c.}) \\
&+(\operatorname{Tr}[M_2(22)M_2^*(23)M_2^*(24)]\exp\{i[\psi_2(22)-\psi_2(23)-\psi_2(24)]\}+\text{c.c}) \\
&+(\operatorname{Tr}[M_2(23)M_2^*(21)M_2^*(25)]\exp\{i[\psi_2(23)-\psi_2(21)-\psi_2(25)]\}+\text{c.c.}) \\
&+(\operatorname{Tr}[M_2(24)M_2(25)M_2(26)]\exp\{i[\psi_2(24)+\psi_2(25)+\psi_2(26)]\}+\text{c.c.})\;. \qquad (19)
\end{aligned}
$$

To evaluate the traces in (19), we use (18) and Table II and define

$$\alpha_0 = -\operatorname{Arccos}(\tfrac{1}{3}) \text{ (second quadrant)}\;. \qquad (20)$$

We obtain

$$
\begin{aligned}
(F_3)_B = -(9\sqrt{3}/128)\beta\epsilon_2^3(2)\{&\cos[3\alpha_0+\psi_2(21)-\psi_2(22)-\psi_2(26)] \\
&+\cos[3\alpha_0+\psi_2(22)-\psi_2(23)-\psi_2(24)]+\cos[3\alpha_0+\psi_2(23)-\psi_2(21)-\psi_2(25)] \\
&+\cos[3\alpha_0+\psi_2(24)+\psi_2(25)+\psi_2(26)]\}\;. \qquad (21)
\end{aligned}
$$

We now turn to the quartic part of the free energy. There are four distinct types of contributions to $(F_4)_B$ which are illustrated in Figs. 7(b)—7(e) and which we calculate separately.

(a) "Single-$\vec{q}$ contribution." This includes Fig. 7(b) and parts of Figs. 7(c) and 7(d). It is simply

$$(F_4)_{B;a} = \frac{1}{(12)^2}2^2\gamma\epsilon_2^4(2)\left[\sum_{n=1}^{6}\operatorname{Tr}[M_2(2n)M_2^*(2n)]\right]^2 = \gamma\epsilon_2^4(2)\;. \qquad (22a)$$

(b) "Two-$\vec{q}$ contribution"; adjacent moment pairs [remainder of Fig. 7(c)]. Using Table II and noting that all such momentum pairs yield identical contributions, we have

$$
\begin{aligned}
(F_4)_{B;b} &= \frac{1}{(12)^2}\frac{6\times 4}{2}2^3\gamma\epsilon_2^4(2)\{\operatorname{Tr}[M_2(21)M_2(22)]\operatorname{Tr}[M_2^*(21)M_2^*(22)] \\
&\qquad +\operatorname{Tr}[M_2(21)M_2^*(22)]\operatorname{Tr}[M_2^*(21)M_2(22)]\} \\
&= \tfrac{41}{192}\gamma\epsilon_2^4(2)\;. \qquad (22b)
\end{aligned}
$$

(c) "Two-$\vec{q}$ contribution"; nonadjacent momentum pairs [remainder of Fig. 7(d)]. We have

$$
\begin{aligned}
(F_4)_{B;c} &= \frac{1}{(12)^2}\frac{6\times 1}{2}2^3\gamma\epsilon_2^4(2)\{\operatorname{Tr}[M_2(21)M_2(24)]\operatorname{Tr}[M_2^*(21)M_2^*(24)] \\
&\qquad +\operatorname{Tr}[M_2(21)M_2^*(24)]\operatorname{Tr}[M_2^*(21)M_2(24)]\} \\
&= \tfrac{1}{48}\gamma\epsilon_2^4(2)\;. \qquad (22c)
\end{aligned}
$$

(d) "Four-$\vec{q}$ contribution" [Fig. 7(e)]. This comes from the closed loops formed by summing four momenta with different indices n. Consider, for example, the loop formed by $(\vec{q}_{21}, -\vec{q}_{23}, -\vec{q}_{24}, -\vec{q}_{26})$. Its contribution is

$$
\begin{aligned}
\frac{1}{(12)^2}2^3\gamma\epsilon_2^4(2)\{&\operatorname{Tr}[M_2(21)M_2^*(24)]\operatorname{Tr}[M_2^*(23)M_2^*(26)]+\operatorname{Tr}[M_2(21)M_2^*(26)] \\
&\times\operatorname{Tr}[M_2^*(23)M_2^*(24)]+\operatorname{Tr}[M_2^*(24)M_2^*(26)]\operatorname{Tr}[M_2^*(23)M_2(21)]\} \\
&\times\exp[\psi_2(21)-\psi_2(23)-\psi_2(24)-\psi_2(26)] \\
&= \tfrac{1}{288}\gamma\epsilon_2^4(2)(1+\tfrac{81}{8}\cos 4\alpha_0)\exp[\psi_2(21)-\psi_2(23)-\psi_2(24)-\psi_2(26)]\;. \qquad (23)
\end{aligned}
$$

The total "four-$\vec{q}$ contribution" is thus

$$(F_4)_{B;d}=\tfrac{1}{144}\gamma\epsilon_2^4(2)(1+\tfrac{81}{8}\cos 4\alpha_0)\{\cos[\psi_2(21)-\psi_2(23)-\psi_2(24)-\psi_2(26)] +\cos[\psi_2(22)-\psi_2(21)-\psi_2(25)-\psi_2(24)] +\cos[\psi_2(23)-\psi_2(22)-\psi_2(26)-\psi_2(25)]\}\ . \tag{22d}$$

The total quartic term is, of course,

$$(F_4)_B=(F_4)_{B;a}+(F_4)_{B;b}+(F_4)_{B;c}+(F_4)_{B;d}\ . \tag{24}$$

Note that only the three linear combinations

$$\begin{aligned}\psi_2(2a)&\equiv\psi_2(21)-\psi_2(22)-\psi_2(26)\ ,\\ \psi_2(2b)&\equiv\psi_2(22)-\psi_2(23)-\psi_2(24)\ ,\\ \psi_2(2c)&\equiv\psi_2(23)-\psi_2(21)-\psi_2(25)\ ,\end{aligned} \tag{25}$$

appear in the expressions for $(F_3)_B$ and $(F_4)_B$. This reflects the invariance of the system free energy with respect to an arbitrary translation or, equivalently, to the location of the origin of our coordination system. From (20), we have $\cos 4\alpha_0=\frac{17}{81}$ and, after summing (17), (21), and (24) and using (9) and (25), we have

$$f_B=\tfrac{1}{4}(t-\kappa^2)\mu_2^2(2)-(27\sqrt{2}/128)\{\cos[3\alpha_0+\psi_2(2a)]+\cos[3\alpha_0+\psi_2(2b)]+\cos[3\alpha_0+\psi_2(2c)] +\cos[3\alpha_0-\psi_2(2a)-\psi_2(2b)-\psi_2(2c)]\}\mu_2^3(2) +(79/64+(25/1152)\{\cos[\psi_2(2a)+\psi_2(2b)]+\cos[\psi_2(2b)+\psi_2(2c)]+\cos[\psi_2(2c)+\psi_2(2a)]\})\mu_2^4(2)\ . \tag{26a}$$

Since $\cos(3\alpha_0)=\frac{23}{27}$, f_B is minimized by choosing $\psi_2(2a)=\psi_2(2b)=\psi_2(2c)=0$. For this choice of phases, the order parameter (16) is invariant under the operations[23] of the bcc space group O^5 ($I432$). We therefore replace the subscript B by O^5 and have

$$f_{O^5}=\tfrac{1}{4}(t-\kappa^2)\mu_2^2(2)-(23\sqrt{2}/32)\mu_2^3(2) +(499/384)\mu_2^4(2)\ . \tag{26b}$$

The I-O^5 thermodynamic transition occurs when

$$f_{O^5}=\partial f_{O^5}/\partial\mu_2(2)=0\ .$$

This gives

$$t_{IO^5}=1587/1996+\kappa^2=0.795+\kappa^2\ . \tag{27}$$

This phase boundary is shown graphically in Fig. 4. Comparing (27) with (13c), we find that for $\kappa\geq 0.939$, the I-O^5 transition occurs before (i.e., at a higher temperature) than the I-C. Thus it is clear that insofar as Landau theory is valid *there must exist one or more nonhelicoidal ordered phases in this region of the phase diagram.*

The change in entropy associated with the I-O^5 phase transition is

$$\begin{aligned}\Delta S_{IO^5}&\equiv 16\,df_{O^5}/dt\,|_{t=t_{IO^5}}=4\mu_2^2(2)\,|_{t=t_{IO^5}}\\ &=2^5\times 3^2\times(23)^2/(499)^2=0.612\ ,\end{aligned} \tag{28}$$

and, for comparison with ΔS_{IC}, is shown in Fig. 5. Also of interest is the ratio of the magnitudes of the order parameters associated with a *single* Fourier component in O^5 and C. At the triple point $t_{IO^5}=t_{IC}$, we have

$$\mu_2(2;O^5)/\sqrt{6}\mu_2(2;C)\,|_{t_{IO^5}=t_{IC}}=0.36\ . \tag{29}$$

While we have found that the O^5 phase has a lower free energy than either the I or C phase for sufficiently large κ and appropriate t, it is clear that C must become the stable configuration when the temperature is sufficiently reduced for all κ. Physically, this is because the low-temperature phase will always be one in which the magnitude of the order parameter is position independent. This is true of C but not O^5. The O^5-C thermodynamic phase boundary $t_{CO^5}(\kappa)$ is found formally by setting

$$\partial f_C/\partial\mu_2=\partial f_C/\partial\mu_0=\partial f_{O^5}/\partial\mu_2=0$$

and $f_C=f_{O^5}$. The resulting set of equations was solved numerically and the results for $t_{O^5C}(\kappa)$ are shown in Fig. 8(a), where the complete I-O^5-C phase diagram is given.

Finally, we have calculated numerally the change in entropy $\Delta S_{O^5C}(\kappa)$ associated with the O^5-C phase transition, using

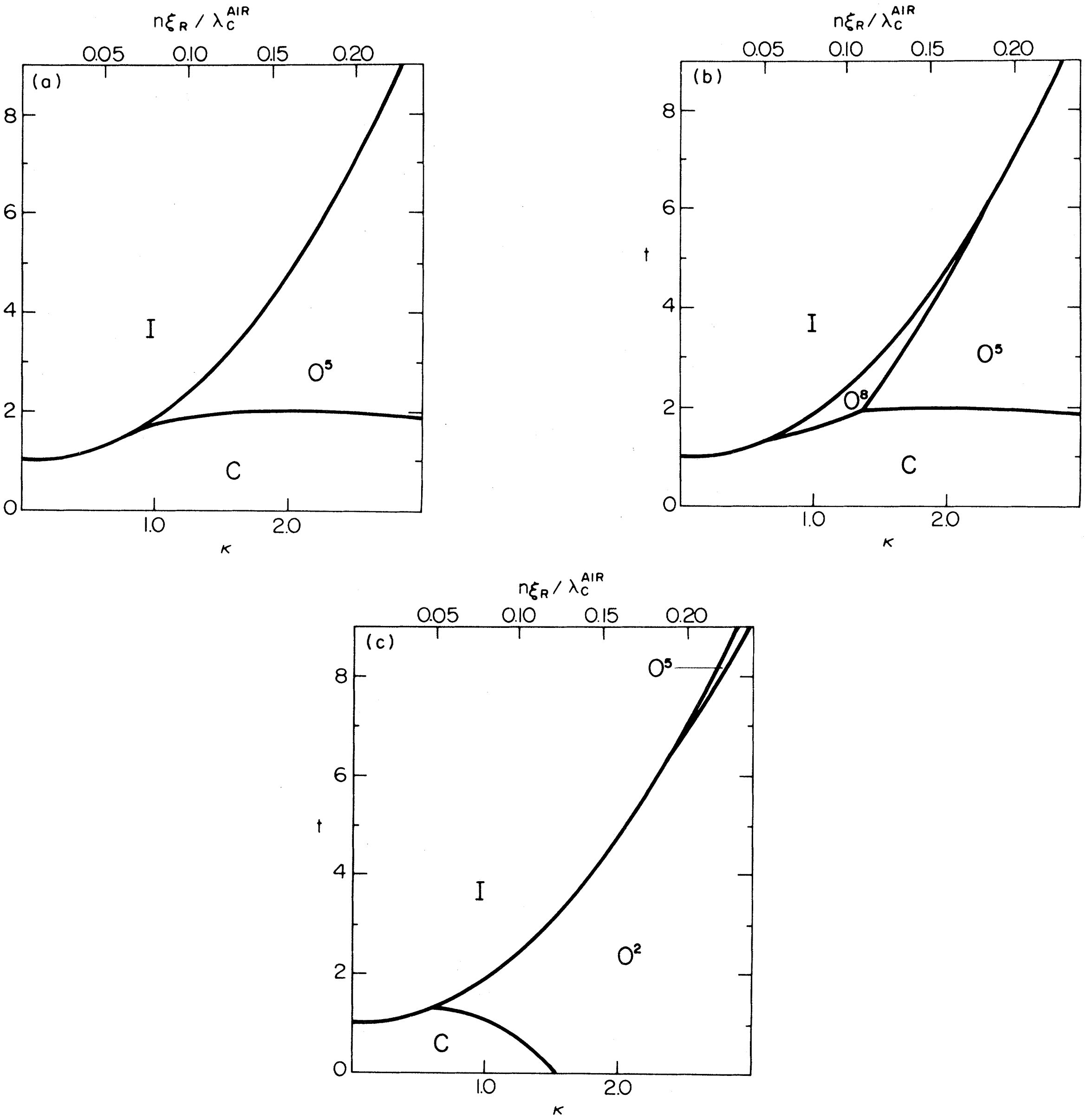

FIG. 8. Theoretical phase diagrams when (a) only I, C, and O^5 phases are allowed, (b) only I, C, O^5, and O^8 phases are allowed, and (c) only I, C, O^2, and O^5 phases are allowed. Here λ_C^{air} is the C-phase Bragg backreflection wavelength in air, n is the index of refraction, and ξ_R is a racemic mixture correlation length at the phase transition. All boundaries shown correspond to first-order phase transitions.

$$\Delta S_{O^5C} = 16(df_C/dt - df_{O^5}/dt)_{t=t_{O^5C}} \; . \qquad (30)$$

The results are shown in Fig. 5.

The order parameter $[\epsilon^{O^5}(\vec{r})]$ defined in (16) can also be written explicitly in real space by noting that, in the cubic coordinate frame,

$$[M_2(21)] = \frac{1}{4}\begin{bmatrix} -1 & 1 & \sqrt{2}i \\ 1 & -1 & -\sqrt{2}i \\ \sqrt{2}i & -\sqrt{2}i & 2 \end{bmatrix} . \qquad (31a)$$

Thus

$$[M_2(21)]e^{i\vec{q}_{21}\cdot\vec{r}}+\text{c.c.}=\frac{1}{2}\begin{bmatrix} -\cos[q_0(x+y)] & \cos[q_0(x+y)] & -\sqrt{2}\sin[q_0(x+y)] \\ \cos[q_0(x+y)] & -\cos[q_0(x+y)] & \sqrt{2}\sin[q_0(x+y)] \\ -\sqrt{2}\sin[q_0(x+y)] & \sqrt{2}\sin[q_0(x+y)] & 2\cos[q_0(x+y)] \end{bmatrix} . \tag{31b}$$

The corresponding expression

$$[M_2(24)]e^{i\vec{q}_{24}\cdot\vec{r}}+\text{c.c.}=\frac{1}{2}\begin{bmatrix} -\cos[q_0(x-y)] & -\cos[q_0(x-y)] & \sqrt{2}\sin[q_0(x-y)] \\ -\cos[q_0(x-y)] & -\cos[q_0(x-y)] & -\sqrt{2}\sin[q_0(x-y)] \\ \sqrt{2}\sin[q_0(x-y)] & -\sqrt{2}\sin[q_0(x-y)] & 2\cos[q_0(x-y)] \end{bmatrix} \tag{31c}$$

is easily found by rotating the tensor in (31b) by π about the y axis of the cubic coordinate system as this is a symmetry element of O^5. Expressions for $[M_2(2n)]\exp[i\vec{q}_{2n}\cdot\vec{r}]$ + c.c for $n=2$, 3, 5, 6 are obtained by cyclic permutations of (31b) and (31c) since [111] is a three-fold symmetry axis in O^5. We then have from (16)

$$\begin{aligned}[\epsilon^{O^5}(\vec{r})]&=[\epsilon_2(2)/\sqrt{12}][A_{52}]\\ &=\frac{\epsilon_2(2)}{\sqrt{12}}\begin{bmatrix} 3c_2c_3-\Sigma_1 & \sqrt{2}s_3(c_1-c_2)-s_1s_2 & \sqrt{2}s_2(c_3-c_1)-s_1s_3 \\ \sqrt{2}s_3(c_1-c_2)-s_1s_2 & 3c_1c_3-\Sigma_1 & \sqrt{2}s_1(c_2-c_3)-s_2s_3 \\ \sqrt{2}s_2(c_3-c_1)-s_1s_3 & \sqrt{2}s_1(c_2-c_3)-s_2s_3 & 3c_1c_2-\Sigma_1 \end{bmatrix}\end{aligned} \tag{32}$$

with

$$\Sigma_1=c_1c_2+c_2c_3+c_1c_3,\quad c_1=\cos(q_0x),\quad s_1=\sin(q_0x),\ \text{etc.}$$

By diagonalizing (32) and putting the resulting matrix in the form given in (15a), the local asymmetry parameter $\eta(\vec{r})$ can be determined. NMR quadrupole splittings in the BP will be discussed in Sec. IV.

D. High-chirality limit: The planar hexagonal phase

As an alternate to the three-dimensional O^5 phase analyzed in Sec. II C, it is possible to envision a two-dimensional hexagonal structure as suggested originally by Brazovskii and Dmitriev.[20] In the high-chirality limit, one would have have only a single triangle [e.g., $(\vec{q}_4, \vec{q}_5, \vec{q}_6)$] of wave vectors with the corresponding order parameter,

$$[\epsilon^{Hx}(r)]=(\tfrac{1}{6})^{1/2}\sum_{n=4}^{6}\epsilon_2(2)([M_2(2n)]\exp\{i[\vec{q}_{2n}\cdot\vec{r}+\psi_2(2n)]\}+\text{c.c.}) . \tag{33}$$

With obvious modifications of (17), (19), (22a), (22b), and (26a), we obtain the reduced free energy

$$\begin{aligned} f_{Hx}=&\ \tfrac{1}{4}(t-\kappa^2)\mu_2^2(2)-\tfrac{27}{32}(\cos\delta)\mu_2^3(2)\\ &+\tfrac{233}{192}\mu_2^4(2) ,\end{aligned} \tag{34}$$

with

$$\delta=3\alpha_0-\psi_2(24)-\psi_2(25)-\psi_2(26) .$$

Clearly, f_{Hx} is minimized by taking $\cos\delta=1$. The *I-Hx* thermodynamic phase transition occurs when

$$f_{Hx}=\partial f_{Hx}/\partial\mu_2(2)=0 ,$$

yielding

$$\begin{aligned} t_{IHx}&=3^7/(2^4\times233)+\kappa^2\\ &=0.587+\kappa^2 .\end{aligned} \tag{35}$$

Comparing (34) with (27) we see that $t_{IHx}<t_{IO^5}$; thus at high chirality the isotropic phase instability can never result in the formation of a two-dimensional hexagonal configuration.

At intermediate chirality, it has been argued[16(b)] that a modified hexagonal structure, in which a $q=0$ nematiclike component is included in $[\epsilon^{Hx}(\vec{r})]$, leads to a region in the phase diagram in which f_{Hx} is lower than f_I, f_{O^5}, and f_C. Of course, including such a component in f_{Hx} while *not* considering allowed $q \neq q_C$ harmonics in other configurations, is not a self-consistent procedure. We shall nevertheless consider briefly this modified hexagonal structure (Hm), in order to show that the conclusion of Kleinert and Maki[16(b)] is incorrect. The modified order parameter is

$$[\epsilon^{Hm}(\vec{r})]=\epsilon_0(O)[M_0(01)]+\frac{1}{\sqrt{6}}\sum_{n=4}^{6}\epsilon_2(2)([M_2(2n)]\exp\{i[\vec{q}_{2n}\cdot\vec{r}+\psi_2(2n)]\}+\text{c.c.})\ , \tag{36}$$

where

$$[M_0(01)]=\frac{1}{\sqrt{6}}\begin{bmatrix}-1 & 0 & 0\\ 0 & -1 & 0\\ 0 & 0 & 2\end{bmatrix} \tag{37a}$$

in a local coordinate system with its polar axis along [111]. In dyadic notation, we write[20]

$$[M_0]_{\alpha\beta}=(3\zeta_\alpha\zeta_\beta-\delta_{\alpha\beta})/\sqrt{6}\ ,$$

and take

$$\hat{\zeta}(01)=(\hat{x}+\hat{y}+\hat{z})/\sqrt{3}\ .$$

The quadratic part of the free energy [see (4) and (5)] is simply

$$(F_2)_{Hm}=\tfrac{1}{2}a\epsilon_0^2(0)+\tfrac{1}{2}(a-d^2/c_1)\epsilon_2^2(2)\ . \tag{38}$$

The cubic contribution is composed of three terms:

$$\begin{aligned}(F_3)_{Hm;a}&=-(3!)2(\tfrac{1}{6})^{3/2}\beta\epsilon_2^2(2)\mathrm{Tr}[M_2(24)M_2(25)M_2(26)]\\ &=-(9\sqrt{6}/64)\beta\epsilon_2^3(2)\cos\delta\ ,\end{aligned} \tag{39a}$$

$$\begin{aligned}(F_3)_{Hm;b}&=-(3!)3(\tfrac{1}{6})\beta\epsilon_0(0)\epsilon_2^2(2)\mathrm{Tr}[M_0(01)M_2(21)M_2^*(21)]\\ &=-(\sqrt{6}/4)\beta\epsilon_0(0)\epsilon_2^2(2)\ ,\end{aligned} \tag{39b}$$

and

$$(F_3)_{Hm;c}=-\beta\epsilon_0^3(0)\mathrm{Tr}[M_0^3(01)]=-(\sqrt{6}/6)\beta\epsilon_0^3(0)\ . \tag{39c}$$

Summing, we have

$$(F_3)_{Hm}=-(1/\sqrt{6})\beta[(27/32)(\cos\delta)\epsilon_2^3(2)+(3/2)\epsilon_0(0)\epsilon_2^2(2)+\epsilon_0^3(0)]\ . \tag{40}$$

The quartic contribution is composed of the following.

(a) "Single-$\vec{q}$ contribution." This is simply

$$\begin{aligned}(F_4)_{Hm;a}&=\gamma\left[\epsilon_0^2(0)\mathrm{Tr}[M_0^2(01)]+\frac{1}{6^2}2^2\epsilon_2^2(2)\sum_{n=4}^{6}\mathrm{Tr}[M_2(2n)M_2^*(2n)]\right]^2\\ &=\gamma(\epsilon_0^2(0)+\epsilon_2^2(2))^2\ .\end{aligned} \tag{41a}$$

(b) "Two-$\vec{q}=\vec{q}_{2n}$ contribution." By analogy with (22b) we have

$$(F_4)_{Hm;b}=(41/192)\gamma\epsilon_2^4(2)\ . \tag{41b}$$

(c) "Two-$\vec{q}$ contribution," with one $\vec{q}=\vec{q}_{2n}$ while the second is $q=0$. We have

$$\begin{aligned}(F_4)_{Hm;c}&=\tfrac{1}{6}\times3\times2^3\gamma\epsilon_0^2(0)\epsilon_2^2(2)\mathrm{Tr}[M_0(01)M_2(21)]\mathrm{Tr}[M_0(01)M_2^*(21)]\\ &=(3/2)\gamma\epsilon_0^2(0)\epsilon_2^2(2)\ .\end{aligned} \tag{41c}$$

(d) "Four-$\vec{q}$ contribution," from four distinct $\vec{q}$ vectors. We have

$$(F_4)_{Hm;d}=(\tfrac{1}{6})^{3/2}(4!)2\gamma\epsilon_0(0)\epsilon_2^3(2)\mathrm{Tr}[M_0(01)M_2(24)]\mathrm{Tr}[M_2(25)M_2(26)]\cos\delta$$
$$=-(9/8)\gamma\epsilon_0(0)\epsilon_2^3(2)\cos\delta\ . \qquad (41\mathrm{d})$$

As before, F_{Hm} is minimized by setting $\cos\delta=1$. Using (9), we obtain for the reduced free energy of the modified hexagonal configuration

$$f_{Hm}=\tfrac{1}{4}t\mu_0^2(0)+\tfrac{1}{4}(t-\kappa^2)\mu_2^2(2)-(27/32)\mu_2^3(2)-(3/2)\mu_0(0)\mu_2^2(2)-\mu_0^3(0)+(233/192)\mu_2^4(2)$$
$$+(9/8)\mu_0(0)\mu_2^3(2)+(7/2)\mu_0^2(0)\mu_2^2(2)+\mu_0^4(0)\ . \qquad (42\mathrm{a})$$

The thermodynamic phase boundary t_{IHm} is found by setting $f_{Hm}=\partial f_{Hm}/\partial\mu_0(0)=\partial f_{Hm}/\partial\mu_2(2)=0$. Alternately, we can again introduce the polar variables (μ,θ) and rewrite (42a) in the form

$$f_{Hm}=\tfrac{1}{4}(t-\kappa^2\cos^2\theta)\mu^2-[(27/32)\cos^3\theta+(3/2)\sin\theta\cos^2\theta+\sin^3\theta]\mu^3$$
$$+[(233/192)\cos^4\theta+(9/8)\sin\theta\cos^3\theta+(7/2)\sin^2\theta\cos^2\theta+\sin^4\theta]\mu^4\ . \qquad (42\mathrm{b})$$

Rather than setting $f_{Hm}=\partial f_{Hm}/\partial\mu=\partial\mu=\partial f_{Hm}/\partial\theta=0$ to determine t_{IHm}, it is simpler numerically to set only $f_{Hm}=\partial f_{Hm}/\partial\mu=0$ and seek the extremum of the resulting equation. We then have

$$t_{IHm}=\max(f_3^2/f_4+\kappa^2\cos^2\theta)\ , \qquad (43\mathrm{a})$$

where

$$f_3(\theta)=(27/32)\cos^3\theta+(3/2)\sin\theta\cos^2\theta+\sin^3\theta\ ,$$

$$f_4(\theta)=(233/192)\cos^4\theta+(9/8)\sin\theta\cos^3\theta$$
$$+(7/2)\sin^2\theta\cos^2\theta+\sin^4\theta\ . \qquad (43\mathrm{b})$$

Note that the local maximum we seek in (43a) is *not* that at $\theta=\pi/2$ ($\mu_2=0$), which describes the nematic phase.

Equation (43a) is easily solved numerically and the results are shown in Fig. 4. We find that t_{IHm} is *always* less than either t_{IC} (for $\kappa\leq 0.939$) or t_{IO^5} (for $\kappa\geq 0.939$). Thus the thermodynamic instability of the disordered phase will *not, within the model framework discussed here,* result in an ordered phase having a two-dimensional hexagonal structure. One can, of course, still inquire as to whether the *Hm* structure is thermodynamically stable in some lower temperature region, i.e., whether f_{Hm} is ever lower than both f_C and f_{O^5}. Numerical analysis of (10), (26b), and (42b) shows that this is not the case as, for both $\kappa<0.939$, $t<t_{IC}$ and $\kappa>0.939$, $t<t_{IO^5}$, *one* of the inequalities $f_C<f_{Hm}$ or $f_{O^5}<f_{Hm}$ is *always* satisfied. The free energies are, of course, compared at their respective thermodynamic equilibrium values.

III. ROLE OF HARMONICS

A. Selection rules

In Sec. II, we showed that, at least for $\kappa>0.939$, there *must* exist an intermediate phase (or phases) between the isotropic and usual cholesteric phases. However, our analysis was based on a model which, strictly speaking, is valid only in the $\kappa\rightarrow\infty$ limit where only a *single* spatial frequency appears in the structure factor. For finite chirality, however, additional spatial frequencies (harmonics) are allowed and, in fact, are observed as additional Bragg reflections. These harmonics have two important consequences. (1) The primary BP Bragg reflection does not appear at the same wavelength as the *C*-phase reflection [see Eq. (5)]. (2) Other cubic structures can have lower free energies than O^5 in regions of the (κ,t) plane.

In order to include spatial harmonics in the Landau free energy in a systematic way, it is useful to first determine the allowed spatial frequencies for any given structure. That is, we are interested in deriving the optical analogue of the structure factor commonly used in the analysis of elastic scattering by x rays.[23] In the latter case, the high energy of the incident radiation results in purely *scalar* scattering,

TABLE III. Optical structure factor for chiral body-centered cubic space groups. $S(W)$ denotes a strong (weak) Bragg reflection. X-ray selection rules are identical to those for $m=0$.

		$(T^3)^a$	$(T^5)^b$	$(O^5)^c$	$(O^8)^d$
$\frac{1}{2}(h^2+k^2+l^2)$	hkl	m: 2 1 0 −1 −2	m: 2 1 0 −1 −2	m: 2 1 0 −1 −2	m: 2 1 0 −1 −2
1	110	+ + + + + S	+ + + + + S	+ − + − + S	+ − + − + S
2	200	+ − + − + S	+ − + − + S	− − + − − W_0	+ − − − + S
3	211	+ + + + + S	+ + + + + S	+ + + + + S	+ + + + + S
4	220	+ + + + + S	+ + + + + S	+ − + − + S	+ − + − + S
5	310	+ + + + + S	+ + + + + S	+ + + + + S	+ + + + + S
6	222	− − + − − W_0	− − + − − W_0	− − + − − W_0	− − + − − W_0
7	321	+ + + + + S	+ + + + + S	+ + + + + S	+ + + + + S
8					
9	330	+ + + + + S	+ + + + + S	+ + + + + S	+ − + − + S

[a] Selection rules; $h+k+l=2n$; $h00$: $m=\pm2,0$; hhh: $m=0$.

[b] Selection rules; $h+k+l=2n$; $h00$: $m=\pm2,0$; hhh: $m=0$.

[c] Selection rules; $h+k+l=2n$; $h00$: $m=0$; $hh0$: $m=\pm2,0$; hhh: $m=0$.

[d] Selection rules; $h+k+l=2n$; $h00$: $m=\pm2$, $h=4n-2$, $m=0$, $h=4n$; $hh0$: $m=\pm2,0$; hhh: $m=0$.

i.e., the interaction is basically one in which incident radiation is scattered by free electrons. At optical frequencies, on the other hand, the much lower energy of the incident radiation results in scattering, in addition, by *all* components of the tensor order parameter. In other works, the BP structure factor has a tensor rather than scalar character.

As noted in Sec. I, the bulk of the experimental results to date are consistent with the existence of bcc and sc structures in the BP region of the phase diagram. We therefore consider generally *all* noncentrosymmetric bcc and sc structures, obtaining the optical selection rules summarized in Tables III and IV. Note particularly that the selection rules depend upon $[h,k,l;m]$. That is, for an allowed Bragg reflection $[h,k,l]$, the strength of the observed peak is dependent upon the polarization state of the incident radiation.

As an example of how the selection rules in Tables III and IV were obtained, consider the state [2,0,0;2]. As noted previously in (3) an alternate description of this state is

$$(1/6)^{1/2}\epsilon_2(4)(15/32\pi)^{1/2}$$
$$\times\sin^2\theta\{\exp[2i\phi+2iqx+i\psi_2(41)]+\text{c.c.}\}\ , \tag{44}$$

where $\epsilon_2(4)$ and $\psi_2(41)$ are the amplitude and phase associated with this particular state and θ,ϕ are polar and azimuthal angles. For [200], the polar axis is along $\hat{x}$. In the space group O^5 ($I432$) there exists a fourfold symmetry axis parallel to $\hat{x}$. Applying this symmetry element to (44) (i.e., replacing ϕ by $\phi+\pi/2$), we find that the given function is transformed into its negative. Thus the [2,0,0;2] state is *forbidden* in O^5 symmetry. Consider, on the other hand, the space group O^8 ($I4_132$). Here there exists a fourfold *screw* axis parallel to $\hat{x}$, in which the $\pi/2$ rotation is combined with a translation of $\frac{1}{4}$ of a unit cell along $\hat{x}$. Applying this symmetry element to (44) [replacing ϕ by $\phi+\pi/2$ and x by $x+(1/4)(2\pi/q)$] we find that the state function is unchanged. Thus the [2,0,0;2] state is *allowed* for the case of O^8 symmetry.

A full discussion of light scattering in cholesterics will be given elsewhere. However, several conclusions can be reached immediately by inspection of Tables III and IV and Figs. 3(b)—3(d). Consider, for example, a back-scattering experiment using circularly polarized incident light. For O^5 symmetry, the $\langle 200\rangle$ Bragg peak is due to scattering from the $m=0$ state only. *Thus it cannot be sensitive to the sense of the polarized light.* Moreover, this peak is associated with a relatively high-lying state and will necessarily be relatively *weak* in comparison with the $\langle 110\rangle$ peak. For O^8 symmetry, on the other hand, the $\langle 200\rangle$ Bragg peak has $m=\pm2$ contributions. Since the $m=+2$ state is a low-lying one while $m=-2$ lies much higher, *this peak will be sensitive to the sense of the incident radition* and its intensity will be of the same order of magnitude as the primary $\langle 110\rangle$ reflection. Turning to sc structures, we see that in all cases the *third* [here $\langle 111\rangle$] *Bragg peak will be polarization independent and*

TABLE IV. Optical structure factor for chiral simple cubic space groups. $S(W)$ denotes a strong (weak) Bragg reflection. X-ray selection rules are identical to those for $m=0$.

		$(T^1)^a$						$(T^4)^b$						$(O^1)^c$						$(O^2)^d$						$(O^6)^e$						$(O^7)^f$					
$h^2+k^2+l^2$	hkl	m: 2	1	0	−1	−2		m: 2	1	0	−1	−2		m: 2	1	0	−1	−2		m: 2	1	0	−1	−2		m: 2	1	0	−1	−2		m: 2	1	0	−1	−2	
1	100	+	−	+	−	+	S	−	+	−	+	−	W_1	−	−	+	−	−	W_0	+	−	−	−	+	S	−	+	−	−	−	W_1	−	−	−	+	−	W_1
2	110	+	+	+	+	+	S	+	+	+	+	+	S	+	−	+	−	+	S	+	−	+	−	+	S	+	−	+	−	+	S	+	−	+	−	+	S
3	111	−	−	+	−	−	W_0	−	−	+	−	−	W_0	−	−	+	−	−	W_0	−	−	+	−	−	W_0	−	−	+	−	−	W_0	−	−	+	−	−	W_0
4	200	+	−	+	−	+	S	+	−	+	−	+	S	−	−	+	−	−	W_0	−	−	+	−	−	W_0	+	−	−	−	+	S	+	−	−	−	+	S
5	210	+	+	+	+	+	S	+	+	+	+	+	S	+	+	+	+	+	S	+	+	+	+	+	S	+	+	+	+	+	S	+	+	+	+	+	S
6	211	+	+	+	+	+	S	+	+	+	+	+	S	+	+	+	+	+	S	+	+	+	+	+	S	+	+	+	+	+	S	+	+	+	+	+	S
7																																					
8	220	+	+	+	+	+	S	+	+	+	+	+	S	+	−	+	−	+	S	+	−	+	−	+	S	+	−	+	−	+	S	+	−	+	−	+	S
9	221	+	+	+	+	+	S	+	+	+	+	+	S	+	+	+	+	+	S	+	+	+	+	+	S	+	+	+	+	+	S	+	+	+	+	+	S

[a] Selection rules. $h00$: $m=\pm 2,0$; hhh: $m=0$.

[b] Selection rules. $h00$: $m=\pm 1$, $h=2n-1$, $m=\pm 2,0$, $h=2n$; hhh: $m=0$.

[c] Selection rules. $h00$: $m=0$; $hh0$: $m=\pm 2,0$; hhh: $m=0$.

[d] Selection rules. $h00$: $m=\pm 2$, $h=2n-1$, $m=0$, $h=2n$; $hh0$: $m=\pm 2,0$; hhh: $m=0$.

[e] Selection rules. $h00$: $m=\pm 1$, $h=4n-3$, $m=\pm 2$, $h=4n-2$, $m=-1$, $h=4n-1$, $m=0$, $h=4n$; $hh0$: $m=\pm 2,0$; hhh: $m=0$.

[f] Selection rules. $h00$: $m=-1$, $h=4n-3$, $m=\pm 2$, $h=4n-2$, $m=1$, $h=4n-1$, $m=0$, $h=4n$; $hh0$: $m=\pm 2,0$; hhh: $m=0$.

weak. Moreover, the first peak (here $\langle 100\rangle$) will be unobservable in back reflection for space groups T^4, O^6, and O^7 and will be polarization insensitive and weak for O^1. Only for T^1 and O^2 are the first two peaks expected to be of the same order of magnitude.

Summarizing, we see that the selection rules given in Tables III and IV provide a direct and straightforward technique for distinguishing between various bcc and sc structures for the cholesteric BP. In addition, they provide a framework within which a Landau theory calculation of the free energies appropriate to various structures can be carried out for general chirality parameter κ.

B. bcc T^3 and O^8 phases

In the previous section we showed that the [2,0,0;2] state, which is forbidden in the O^5 structure, is allowed for O^8 and T^3. As an example of the role harmonics can play in a Landau free energy calculation of cubic structures, we consider a modified order parameter in which spatial Fourier components are associated with wave vectors of magnitude $\sqrt{2}q$ and $2q$. (Note that now $q \neq q_0$.) As in Sec. II C we associate the former with wave vectors lying along $\langle 110\rangle$ directions as shown in Fig. 6 and listed in Table I. For the latter the wave vectors will belong to $\langle 200\rangle$ with $m=2$ and their labeling and local axis system are summarized in Table V. Using (2), the order parameter for the modified cubic phase is

$$[\epsilon^{Bm}(\vec{r})]=(\tfrac{1}{12})^{1/2}\sum_{n=1}^{6}\epsilon_2(2)([M_2(2n)]\times\exp\{i[\vec{q}_{2n}\cdot\vec{r}+\psi_2(2n)]\}+\text{c.c.})+(\tfrac{1}{6})^{1/2}\sum_{n=1}^{3}\epsilon_2(4)([M_2(4n)]\times\exp\{i[\vec{q}_{4n}\cdot\vec{r}+\psi_2(4n)]\}+\text{c.c.})\qquad(45)$$

TABLE V. Wave vectors and local axis systems $(\hat{\xi},\hat{\eta},\hat{\zeta})$ for $\langle 200\rangle$ wave vectors. For the wave vectors $-\vec{q}_{4n}$, $\hat{\eta}_{4n}$ is replaced by $-\hat{\eta}_{4n}$. The wave vector q is determined, in general, from (5).

Wave vector ($\vec{q}_{4n}=2q\hat{\zeta}_{4n}$)	$\hat{\xi}_{4n}$	$\hat{\eta}_{4n}$
$\vec{q}_{41}=2q\hat{x}$	$\hat{y}$	$\hat{z}$
$\vec{q}_{42}=2q\hat{y}$	$\hat{z}$	$\hat{x}$
$\vec{q}_{43}=2q\hat{z}$	$\hat{x}$	$\hat{y}$

with $q_{4n}=\sqrt{2}q_{2n}=2q$. Using (4) and (5), the quadratic part of the Landau free energy becomes

$$
\begin{aligned}
(F_2)_{Bm}=\tfrac{1}{2}\{ & [a-d_1^2/c_1+(d_1^2/c_1)(r-1)^2]\epsilon_2^2(2) \\
& +[a-d_1^2/c_1+(d_1^2/c_1)(\sqrt{2}r-1)^2]\epsilon_2^2(4)\}
\end{aligned}
\tag{46}
$$

with

$$
r=[\epsilon_2^2(2)+\sqrt{2}\epsilon_2^2(4)]/[\epsilon_2^2(2)+2\epsilon_2^2(4)]\ . \tag{47}
$$

Turning to the cubic part of the free energy, we have two contributions, one of which, $(F_3)_{Bm;a}$ [proportional to $\epsilon_2^3(2)$], has been calculated in Sec. II C and is given explicitly in (21). The new contribution will be proportional to $\epsilon_2^2(2)\epsilon_2(4)$ and is given by

$$
\begin{aligned}
(F_3)_{Bm;b}= & -3!(\tfrac{1}{12})(\tfrac{1}{6})^{1/2}\beta\epsilon_2^2(2)\epsilon_2(4) \\
& \times\sum_{n=1}^{3}\{[\,\mathrm{Tr}[M(2n)M(2(n+3))M^*(4(n+1))] \\
& \qquad\times\exp\{i[\psi_2(2n)+\psi_2(2(n+3))-\psi_2(4(n+1))]\}+\text{c.c.}] \\
& \qquad+[\,\mathrm{Tr}[M(2n)M^*(2(n+3))M(4n)]\exp\{i[\psi_2(2n)-\psi_2(2(n+3))+\psi_2(4n)]\}+\text{c.c.}]\}\ , \\
= & -(\sqrt{6}/96)(3+2\sqrt{2})\beta\epsilon_2^2(2)\epsilon_2(4) \\
& \times\sum_{n=1}^{3}\{\cos[\psi_2(2n)+\psi_2(2(n+3))-\psi_2(4(n+1))]\ -\cos[\psi_2(2n)-\psi_2(2(n+3))-\psi_2(4n)]\}\ .
\end{aligned}
\tag{48}
$$

The index $n+1$ in (48) is defined modulo 3. Turning to the quartic contributions, we have four distinct types.
(a) "Single-$\vec{q}$ contribution." This is simply

$$
(F_4)_{Bm;a}=\gamma[\epsilon_2^2(2)+\epsilon_2^2(4)]^2\ . \tag{49a}
$$

(b) "Two-$\vec{q}$ contribution." Including the part proportional to $\epsilon_2^4(2)$ and given previously in (22b) and (22c), we have

$$
\begin{aligned}
(F_4)_{Bm;b}= & \gamma(\tfrac{41}{192}+\tfrac{1}{48})\epsilon_2^4(2)+\frac{1}{12\times 6}2^3\epsilon_2^2(2)\epsilon_2^2(4) \\
& \times\sum_{n=1}^{6}\sum_{m=1}^{3}\{[\mathrm{Tr}[M_2(2n)M_2(4m)]\,\mathrm{Tr}[M_2^*(2n)M_2^*(4m)] \\
& \qquad+\mathrm{Tr}[M_2(2n)M_2^*(4m)]\,\mathrm{Tr}[M_2^*(2n)M_2(4m)]\} \\
& +\frac{1}{6^3}2^3\epsilon_2^4(4)\sum_{n,m=1}^{3}\{\mathrm{Tr}[M_2(4n)M_2(4m)]\,\mathrm{Tr}[M_2^*(4n)M_2^*(4m)] \\
& \qquad+\mathrm{Tr}[M_2(4n)M_2^*(4m)]\,\mathrm{Tr}[M_2(4n)M_2(4m)]\} \\
= & \gamma[\tfrac{15}{64}\epsilon_2^4(2)+\tfrac{19}{24}\epsilon_2^2(2)\epsilon_2^2(4)+\tfrac{1}{2}\epsilon_2^4(4)]\ .
\end{aligned}
\tag{49b}
$$

(c) "Three-$\vec{q}$ contribution." This is given by

$$(F_4)_{Bm;c} = \gamma \frac{1}{12\times 6} 2^3 \epsilon_2^2(2)\epsilon_2^2(4)$$

$$\times \sum_{n=1}^{3} \{[\mathrm{Tr}[M_2(2n)M_2^*(4n)]\,\mathrm{Tr}[M_2(2n)M_2^*(4(n+1))]$$

$$\times \exp\{i[2\psi_2(2n)-\psi_2(4n)-\psi_2(4(n+1))]\}+\mathrm{c.c.}]$$

$$+[\mathrm{Tr}[M_2(2(n+3))M_2(4n)]\,\mathrm{Tr}[M_2(2(n+3))M_2^*(4(n+1))]$$

$$\times \exp\{i[2\psi_2(2(n+3))+\psi_2(4n)-\psi_2(4(n+1))]\}+\mathrm{c.c.}]\}$$

$$= -\gamma\epsilon_2^2(2)\epsilon_2^2(4)[(17+12\sqrt{2})/288] \sum_{n=1}^{3} \{\cos[2\psi_2(2n)-\psi_2(4n)-\psi_2(4(n+1))]$$

$$+\cos[2\psi_2(2(n+3))+\psi_2(4n)-\psi_2(4(n+1))]\}\ , \tag{49c}$$

where the index $n+1$ is again defined modulo 3.

(d) "Four-$\vec{q}$ contribution." In addition to the contribution $(F_4)_{Bm;d}$ [proportional to $\epsilon_2^4(2)$] calculated in Sec. II C and given explicitly in (22d); we have additional terms due to the closed loops formed by the summing of four momenta, three with $\sigma=2$ and different n, and one with $\sigma=4$. Consider, for example, the loop formed by $(\vec{q}_{21}, \vec{q}_{25}, \vec{q}_{26}, -\vec{q}_{41})$. Its contribution is

$$(\tfrac{1}{12})^{3/2}(\tfrac{1}{6})^{1/2}2^3\gamma\epsilon_2^3(2)\epsilon_2(4)\{\mathrm{Tr}[M_2(21)M_2(25)]\,\mathrm{Tr}[M_2(26)M_2^*(41)]$$

$$+\mathrm{Tr}[M_2(21)M_2(26)]\,\mathrm{Tr}[M_2(25)M_2^*(41)]$$

$$+\mathrm{Tr}[M_2(21)M_2^*(41)]\,\mathrm{Tr}[M_2(25)M_2(26)]\}$$

$$\times \exp\{i[\psi_2(21)+\psi_2(25)+\psi_2(26)-\psi_2(41)]\}$$

$$=\gamma\epsilon_2^3(2)\epsilon_2(4)(i/1152)(24+17\sqrt{2})\exp\{i[\psi_2(21)+\psi_2(25)+\psi_2(26)-\psi_2(41)]\}\ . \tag{50}$$

There are 12 terms of this type and their total contribution is given by

$$(F_4)_{Bm;e} = -\gamma\epsilon_2^3(2)\epsilon_2(4)[(24+17\sqrt{2})/576]$$

$$\times \sum_{n=1}^{3} \{\sin[\psi_2(2n)+\psi_2(2(n+4))+\psi_2(2(n+5))-\psi_2(4n)]$$

$$-\sin[\psi_2(2n)-\psi_2(2(n+1))+\psi_2(2(n+2))-\psi_2(4n)]$$

$$+\sin[\psi_2(2(n+2))-\psi_2(2(n+3))-\psi_2(2(n+4))-\psi_2(4n)]$$

$$-\sin[\psi_2(2(n+1))-\psi_2(2(n+3))+\psi_2(2(n+5))-\psi_2(4n)]\}\ . \tag{49d}$$

Here the indices $n+m$ are to be understood as being cyclic in either the set (1,2,3) or (4,5,6). The total quartic term $(F_4)_{Bm}$, obtained by summing (22d) and (49a)–(49d), is

$$(F_4)_{Bm} = (F_4)_{Bm;a} + (F_4)_{Bm;b} + (F_4)_{Bm;c} + (F_4)_{Bm;d} + (F_4)_{Bm;e}\ . \tag{51}$$

Rather than analyzing directly the total free energy F_{Bm} by summing (21), (22d), (46), (48), and (51), we first determine the phases $\psi_2(2n)$ $(n=1,\ldots,6)$ and $\psi_2(4m)$ $(m=1,2,3)$. For a *given* space-group symmetry, these phases are *not* independent of each other and we can use these symmetry constraints to simplify our expressions for the free energy. This if the origin of our coordinate system is set at the point $(\frac{1}{2},\frac{1}{2},0)$ in the O^5 unit cell with point-group symmetry 42, a necessary (though *not* sufficient) condition for O^5 symmetry is that

$$\begin{aligned}&\psi_2(2n)=0 \text{ or } \pi\ ,\quad n=1,\ldots,6\\&\psi_2(4n)=0 \text{ or } \pi\ ,\quad n=1,2,3\ .\end{aligned}\tag{52}$$

Using (52) we find that $(F_3)_{Bm;b}=(F_4)_{Bm;e}=0$ and that F_{Bm} is minimized by setting all phases equal to zero. Using (9), we have

$$\begin{aligned}f_{Bm}=&\tfrac{1}{4}[t-\kappa^2+\kappa^2(r-1)^2]\mu_2^2(2)+\tfrac{1}{4}[t-\kappa^2+\kappa^2(\sqrt{2}r-1)^2]\mu_2^2(4)-(23\sqrt{2}/32)\mu_2^3(2)\\&+(449/384)\mu_2^4(2)+[(39-4\sqrt{2})/16]\mu_2^2(2)\mu_2^2(4)+(13/12)\mu_2^4(4)\ .\end{aligned}\tag{53}$$

A necessary condition for O^5 symmetry, as discussed in Sec. III A, is $\mu_2(4)=0$. The free energy (53) satisfies this condition for $t\geq t_{O^5T^3}$, where

$$\begin{aligned}t_{O^5T^3}=&2(\sqrt{2}-1)\kappa^2\\&-[(39-4\sqrt{2})/4]\mu_2^2(2)\ .\end{aligned}\tag{54}$$

For $t\leq t_{O^5T^3}$, $\mu_2(4)\neq 0$ and (53) is relevant to a phase having T^3 ($I23$) rather than O^5 symmetry. Equation (54) therefore gives the O^5-T^3 second-order phase boundary, since $\mu_2(4)=0$ and $r=1$ at $t_{O^5T^3}(\kappa)$. The value of μ_2 in (54) is determined from (26b) by setting $\partial f_{O^5}/\partial\mu_2=0$ at $t=t_{O^5T^3}$. Numerical calculation shows that $t_{O^5T^3}<t_{O^5C}$ for $0\leq\kappa\leq 10$ and thus T^3 is not relevant within the framework considered here.

Consider now a system having O^8 ($I4_132$) symmetry.[23] We take as our origin the point $(\frac{3}{8},\frac{3}{8},\frac{3}{8})$ having point symmetry 32. Applying various operations of O^8, we find that

$$\begin{aligned}&\psi_2(2n)=0 \text{ or } \pi\ ,\ \text{for } n=1,2,3\\&\psi_2(2n)=\pm\pi/2\ ,\ \text{for } n=4,5,6\\&\psi_2(4n)=\pm\pi/2\ ,\ \text{for } n=1,2,3\ .\end{aligned}\tag{55a}$$

To minimize the free energy, we take

$$\begin{aligned}&\psi_2(21)=0\ ,\\&\psi_2(41)=\psi_2(24)=-\pi/2\ .\end{aligned}\tag{55b}$$

Note from (20) that $\sin 3\alpha_0=-10\sqrt{2}/27$ and using the normalized amplitudes given in (9), we have

$$\begin{aligned}f_{O^8}=&\tfrac{1}{4}[t-\kappa^2+\kappa^2(r-1)^2]\mu_2^2(2)+\tfrac{1}{4}[t-\kappa^2+\kappa^2(\sqrt{2}r-1)^2]\mu_2^2(4)-\tfrac{5}{8}\mu_2^3(2)\\&-\tfrac{3}{8}(3+2\sqrt{2})\mu_2^2(2)\mu_2(4)+\tfrac{449}{384}\mu_2^4(2)+[(151+12\sqrt{2})/48]\mu_2^2(2)\mu_2^2(4)\\&+[(24+17\sqrt{2})/48]\mu_2^3(2)\mu_2(4)+\tfrac{13}{12}\mu_2^4(4)\ .\end{aligned}\tag{56}$$

The I-O^8 thermodynamic phase transition occurs at

$$f_{O^8}=\partial f_{O^8}/\partial\mu_2(2)=\partial f_{O^8}/\partial\mu_2(4)=\partial f_{O^8}/\partial r=0\ .$$

The resulting set of equations was solved numerically to determine $t_{IO^8}(\kappa)$. The results are shown in Fig. 8(b) where we also give $t_{O^8O^5}$ and t_{O^8C}, the phase boundaries between the O^8 and O^5 and the O^8 and C phases, respectively. *The effect of including [2,0,0;2] states in the order parameter thus results in the appearance of a new bcc phase for intermediate values of* κ. Unlike O^5, the O^8 structure is nonsymmorphic and has no isotropic (defect) points.

The entropy changes associated with the phase boundaries shown in Fig. 8(b) are given in Fig. 5. In addition, at the triple point $t_{IO^8}=t_{IC}$, we find for the order-parameter component magnitude ratios

$$\mu_2(2;O^8)/\sqrt{6}\mu_2(2;C)=0.32\ ,\tag{57a}$$

$$\mu_2(4;O^8)/\sqrt{3}\mu_2(2;C)=0.20\ ,\tag{57b}$$

and, using (47), for the shift in the position of the $\langle 110 \rangle$ Bragg reflection

$$r(O^8)=0.91\ . \tag{58}$$

As discussed in Sec. II C for O^5, we can also write $[\epsilon^{O^8}(\vec{r})]$ explicitly in real space. Using (55b) and shifting our origin to the standard one,[23] we have

$$[\epsilon^{O^8}(\vec{r})]=[\epsilon_2(2)/\sqrt{12}][A_{82}]+[\epsilon_2(4)/\sqrt{6}][A_{84}] \tag{59a}$$

with

$$[A_{82}]=\begin{bmatrix} \Sigma_2-3s_2c_3 & \sqrt{2}(c_1c_3+s_2s_3)-s_2c_1 & \sqrt{2}(c_3c_2+s_1s_2)-s_1c_3 \\ \sqrt{2}(c_1c_3+s_2s_3)-s_2c_1 & \Sigma_2-3s_3c_1 & \sqrt{2}(c_2c_1+s_3s_1)-s_3c_2 \\ \sqrt{2}(c_3c_2+s_1s_2)-s_1c_3 & \sqrt{2}(c_2c_1+s_3s_1)-s_3c_2 & \Sigma_2-3s_1c_2 \end{bmatrix}, \tag{59b}$$

$$[A_{84}]=\begin{bmatrix} c_3'-c_2' & -s_3' & -s_2' \\ -s_3' & c_1'-c_3' & -s_1' \\ -s_2' & -s_1' & c_2'-c_1' \end{bmatrix}, \tag{59c}$$

with $\Sigma_2=s_1c_2+s_2c_3+s_3c_1$, $c_1=\cos(qx)$, $s_1=\sin(qx)$, $c_1'=\cos(2qx)$, $s_1'=\sin(2qx)$, etc. As before, the local asymmetry parameter $\eta(\vec{r})$ can be found by diagonalizing $[\epsilon^{O^8}(\vec{r})]$ and comparing the resulting matrix with (15a).

C. sc O^2 phase

In this section we consider a different modification of the basic O^5 structure analyzed in Sec. II C. We introduce a *subharmonic,* whose spatial Fourier components are associated with wave vectors of magnitude q. These wave vectors belong to the set $\langle 100 \rangle$ with $m=2$ and their local axis systems are identical with those already given in Table V for $\langle 200 \rangle$. As is clear from Fig. 6 and Table IV these Fourier components destroy bcc translational invariance and the resulting structure is sc.[12(e),13] The relevant order parameter is

$$\begin{aligned}[\epsilon^{S}(\vec{r})]=&(\tfrac{1}{6})^{1/2}\sum_{n=1}^{3}\epsilon_2(1)([M_2(1n)]\exp\{i[\vec{q}_{1n}\cdot\vec{r}+\psi_2(1n)]\}+\text{c.c.})\\ &+(\tfrac{1}{12})^{1/2}\sum_{n=1}^{6}\epsilon_2(2)([M_2(2n)]\exp\{i[\vec{q}_{2n}\cdot\vec{r}+\psi_2(2n)]\}+\text{c.c.})\ ,\end{aligned} \tag{60}$$

with $q_{1n}=q_{2n}/\sqrt{2}=q$. Using (4) and (5), the quadratic part of the Landau free energy is

$$(F_2)_S=\tfrac{1}{2}\{[a-d_1^2/c_1+(d_1^2/c_1)(r/\sqrt{2}-1)^2]\epsilon_2^2(1)+[a-d_1^2/c_1+(d_1^2/c_1)(r-1)^2]\epsilon_2^2(2)\}\ , \tag{61}$$

with

$$r=\sqrt{2}[\epsilon_2^2(1)+\sqrt{2}\epsilon_2^2(2)]/[\epsilon_2^2(1)+2\epsilon_2^2(2)]\ . \tag{62}$$

There are two cubic contributions, one of which, $(F_3)_{S;a}$, is proportional to $\epsilon_2^3(2)$ and is given by (21). The second part is

$$\begin{aligned}(F_3)_{S;b}=&3!(\tfrac{1}{6})(\tfrac{1}{12})^{1/2}\beta\epsilon_2^2(1)\epsilon_2(2)\\ &\times\sum_{n=1}^{3}\{[\text{Tr}[M_2(1n)M_2(1(n+1))M_2^*(2n)]\\ &\qquad\times\exp\{i[\psi_2(1n)+\psi_2(1(n+1))-\psi_2(2n)]\}+\text{c.c.}]\\ &\qquad+[\text{Tr}[M_2(1n)M_2^*(1(n+1))M_2(2(n+3))]\\ &\qquad\times\exp\{i[\psi_2(1n)-\psi_2(1(n+1))+\psi_2(2(n+3))\}+\text{c.c.}]\}\\ =&[\sqrt{3}(3+2\sqrt{2})/48]\beta\epsilon_2^2(1)\epsilon_2(2)\sum_{n=1}^{3}\{\cos[\psi_2(1n)+\psi_2(1(n+1))-\psi_2(2n)]\\ &\qquad+\cos[\psi_2(1n)-\psi_2(1(n+1))+\psi_2(2(n+3))]\}\ ,\end{aligned} \tag{63}$$

where the index $n+1$ in (63) is defined modulo 3.

The quartic term contains contributions proportional to $\epsilon_2^4(1)$, $\epsilon_2^4(2)$, and $\epsilon_2^2(1)\epsilon_2^2(2)$. Noting that the contribution proportional to $\epsilon_2^4(1)$ is identical to that proportional to $\epsilon_2^4(4)$ which was calculated in Sec. III B, we have from (49a) and (49b)

$$(F_4)_{S;a}=\tfrac{13}{12}\gamma\epsilon_2^4(1)\ . \tag{64a}$$

The $\epsilon_2^4(2)$ contribution is simply

$$(F_4)_{S;b}=(F_4)_B\ , \tag{64b}$$

and is given by (24). The final contribution, $\epsilon_2^2(1)\epsilon_2^2(2)$, is composed of "single-$\vec{q}$," "two-$\vec{q}$," "three-$\vec{q}$," and "four-$\vec{q}$" terms. The first two are identical to those calculated for the case of $\epsilon_2^2(2)\epsilon_2^2(4)$ in Sec. III B and, from (49a) and (49b), we have

$$\begin{aligned}(F_4)_{S;c}&=\gamma[2+(19/24)]\epsilon_2^2(1)\epsilon_2^2(2)\\&=(67/24)\gamma\epsilon_2^2(1)\epsilon_2^2(2)\ .\end{aligned} \tag{64c}$$

The "three-$\vec{q}$" term is given by

$$\begin{aligned}(F_4)_{S;d}={}&\gamma\frac{1}{12\times 6}2^3\epsilon_2^2(1)\epsilon_2^2(2)\\&\times\sum_{n=1}^{3}\{[\mathrm{Tr}[M_2(1n)M_2^*(2n)]\,\mathrm{Tr}[M_2(1n)M_2(2(n+3))]\\&\qquad\times\exp\{i[2\psi_2(1n)-\psi_2(2n)+\psi_2(2(n+3))]\}+\text{c.c.}]\\&\qquad+[\mathrm{Tr}[M_2(1n)M_2^*(2(n+2))]\,\mathrm{Tr}[M_2(1n)M_2^*(2(n+5))]\\&\qquad\times\exp\{i[2\psi_2(1n)-\psi_2(2(n+2))-\psi_2(2(n+5))]\}+\text{c.c.}]\}\\={}&\gamma\epsilon_2^2(1)\epsilon_2^2(2)[(17+12\sqrt{2})/288]\sum_{n=1}^{3}\{\cos[2\psi_2(1n)-\psi_2(2n)+\psi_2(2(n+3))]\\&\qquad+\cos[2\psi_2(1n)-\psi_2(2(n+2))-\psi_2(2(n+5))]\}\ ,\end{aligned} \tag{64d}$$

where all indices are to be understood as being cyclic in either the set (1,2,3) or (4,5,6).

The "four-$\vec{q}$" term is due to closed loops formed by the summing of four distinct momenta, two with $\sigma=1$ and two with $\sigma=2$. Consider, for example, the loop formed by $(\vec{q}_{11}, \vec{q}_{12}, -\vec{q}_{22}, -\vec{q}_{26})$. We have

$$\begin{aligned}&(\tfrac{1}{6})(\tfrac{1}{12})2^3\gamma\epsilon_2^2(1)\epsilon_2^2(2)\{\mathrm{Tr}[M_2(11)M_2(12)]\,\mathrm{Tr}[M_2^*(22)M_2^*(26)]\\&\qquad+\mathrm{Tr}[M_2(11)M_2^*(22)]\,\mathrm{Tr}[M_2(12)M_2^*(26)]\\&\qquad+\mathrm{Tr}[M_2(11)M_2^*(26)]\,\mathrm{Tr}[M_2(12)M_2^*(22)]\}\\&\qquad\times\exp\{i[\psi_2(11)+\psi_2(12)-\psi_2(22)-\psi_2(26)]\}\ ,\\&\qquad=-\gamma\epsilon_2^2(1)\epsilon_2^2(2)[(9e^{2i\alpha_0}+13+12\sqrt{2})/576]\exp\{i[\psi_2(11)+\psi_2(12)+\psi_2(22)-\psi_2(26)]\}\ .\end{aligned} \tag{65}$$

There are 24 terms of this type and their total contribution is

$$\begin{aligned}(F_4)_{S;e}=-\gamma\epsilon_2^2(1)\epsilon_2^2(2)\Bigg[&[(1+2\sqrt{2})/48]\\ &\times\sum_{n=1}^{3}\{\cos[\psi_2(1n)+\psi_2(1(n+1))-\psi_2(2(n+1))-\psi_2(2(n+5))]\\ &\quad+\cos[\psi_2(1n)+\psi_2(1(n+1))-\psi_2(2(n+2))+\psi_2(2(n+4))]\\ &\quad+\cos[\psi_2(1n)-\psi_2(1(n+1))-\psi_2(2(n+4))-\psi_2(2(n+5))]\\ &\quad+\cos[\psi_2(1n)-\psi_2(1(n+1))+\psi_2(2(n+1))-\psi_2(2(n+2))]\}\\ &+(\sqrt{2}/72)\sum_{n=1}^{3}\{\text{as above, }\cos\Longrightarrow\sin\}\Bigg]\ ,\end{aligned}\tag{64e}$$

with the same index convention. The total quartic term $(F_4)_S$ is obtained by summing (64a)–(64e).

Setting the origin of our coordinate system at the point (0,0,0) in the O^2 ($P4_232$) unit cell,[23] we find that the phases must satisfy

$$\begin{aligned}&\psi_2(1n)=0 \text{ or } \pi\ ,\quad n=1,2,3\\ &\psi_2(2n)=0 \text{ or } \pi\ ,\quad n=1,\ldots,6\ .\end{aligned}\tag{66}$$

The free energy F_{O^2} is minimized by choosing $\psi_2(2n)=\pi$ for all n. Using (9), (21), (59), (61), (62a)–(62e), and (64) then gives

$$\begin{aligned}f_{O^2}=&\tfrac{1}{4}[t-\kappa^2+\kappa^2(r/\sqrt{2}-1)^2]\mu_2^2(1)+\tfrac{1}{4}[t-\kappa^2+\kappa^2(r-1)^2]\mu_2^2(2)\\ &-[3(4+3\sqrt{2})/8]\mu_2^2(1)\mu_2(2)+(23\sqrt{2}/32)\mu_2^3(2)+(13/12)\mu_2^4(1)\\ &+[(139-12\sqrt{2})/48]\mu_2^2(1)\mu_2^2(2)+(499/384)\mu_2^4(2)\ .\end{aligned}\tag{67}$$

The I-O^2 thermodynamic phase transition temperature $t_{IO^2}(\kappa)$ is determined by setting $f_{O^2}=\partial f_{O^2}/\partial\mu_2(1)=\partial f_{O^2}/\partial\mu_2(2)=\partial f_{O^2}/\partial r=0$. These equations were solved numerically and the result is shown graphically in Fig. 8(c), where the complete phase diagram for the I, O^2, O^5, and C phases is given. *We again find that a modified order parameter results in the appearance of a new, nonsymmorphic phase.* Unlike the case of O^8, however, the new phase is now no longer bcc, but rather sc. A comparison of the O^2 and O^8 phases will be given in the following section.

The entropy changes associated with the phase boundaries of Fig. 8(c) are given in Fig. 5. At the triple point $t_{IO^2}=t_{IC}$, we obtain the order parameter component magnitude ratios

$$\mu_2(1;O^2)/\sqrt{3}\mu_2(2;C)=0.51\ ,\tag{68a}$$

$$\mu_2(2;O^2)/\sqrt{6}\mu_2(2,C)=0.20\ ,\tag{68b}$$

and, using (62), for the shift in the ⟨110⟩ Bragg reflection

$$r(O^2)=1.25\ .\tag{69a}$$

Experimentally, however, the quantity of interest is the shift of the *first* Bragg reflection with respect to that of the C phase. For the case of O^2 this is not r but rather

$$r(O^2)/\sqrt{2}=0.89\ .\tag{69b}$$

In real space, the order parameter $[\epsilon^{O^2}(\vec{r})]$ takes the form

$$[\epsilon^{O^2}(\vec{r})]=[\epsilon_2(1)/\sqrt{6}][A_{21}]+[\epsilon_2(2)/\sqrt{12}][A_{22}]\tag{70a}$$

with

$$[A_{21}]=\begin{bmatrix}c_3-c_2 & -s_3 & -s_2\\ -s_3 & c_1-c_3 & -s_1\\ -s_3 & -s_1 & c_2-c_1\end{bmatrix}\ ,\tag{70b}$$

$$[A_{22}]=-[A_{52}]\ .\tag{70c}$$

The tensor $[A_{52}]$ was given previously in (32). Once again, the local asymmetry parameter is determined by diagonalizing the order-parameter matrix and using (15a).

IV. DISCUSSION

In this paper we have developed the Landau theory of phase transitions in cholesteric systems and shown, within this framework, that the existence of anomolous cubic phases can be understood and their properties studied in detail. In particular, the following experimental results, summarized earlier in Sec. I, follow naturally from the calculations in Secs. II and III.

(1) The narrowing and eventual disappearance of the BP region with increasing pitch.

(2) The narrowness of the BP region. Experimentally, the index of refraction[3] $n \simeq 1.6$, the correlation length (Ref. 24) $\xi_R \simeq 250$ Å, and the C-phase Bragg backreflection is at[1–3,7] $\lambda_C^{\text{air}} = 4000$–$6000$ Å. Thus κ is in the range $0.8 < \kappa < 1.3$ and, from Fig. 8, we see that the BP region should be of the order of unity on our reduced temperature scale. This unit, as noted following (11), is extrapolated-from-the-disordered phase transition temperatures for a racemic mixture. Experimentally, it is (Ref. 25) 0.5–1 K. Thus our model prediction is in excellent agreement with experimental data [see particularly Ref. 7(d)].

(3) The existence of more than one BP. We have seen that the inclusion of harmonics in the order parameter results in cubic structures other than O^5 becoming thermodynamically stable. The Landau theory does not, however, encompass an amorphous phase having the properties of BPIII. A possible explanation for the existence of this anomolous phase has been given elsewhere.[12(g)]

(4) All of the cubic phases (O^2, O^5, O^8) discussed here will exhibit many of the experimentally observed optical properties of both BPI and BPII. These include absence of birefringence, optical activity, and Bragg scattering.

We now give a more detailed comparison of the calculated properties of the O^2, O^5 and O^8 phases with those observed in BPI and BPII. To begin, note that the results of Flack and Crooker[3(b)] rule out any identification of O^5 with either BPI or BPII. In the materials studied, these authors found that the second Bragg line is strongly sensitive to the sense of polarized input light. By using Table III or Fig. 3(b) and noting the discussion in Sec. III A, we conclude[12(d,e)] that neither BPI or BPII can have an O^5 structure. This conclusion also follows from the more limited data of Meiboom and Sammon[2] taken on different compounds.

There remains the O^2 and O^8 structures to be considered. Let us consider the (κ,t) plane phase diagram [Figs. 8(b) and 8(c)]. For the O^2 and O^8 model structures analyzed in Sec. III, we find, for values of κ between 0.6 and 1.4, that t_{IO^2} and t_{IO^8} are equal to within 0.1%. Lacking at this stage a more refined calculation, we can nevertheless make some qualitative predictions. From Tables III and IV or Figs. 3(c) and 3(d), we see that the third and fourth low-lying harmonics [2,1,1;2] and [2,2,0;2] are *allowed* in O^8 while the corresponding [1,1,1;2] and [2,0,0;2] states in O^2 are *forbidden*. Extending our calculation to include these states would therefore necessarily *raise* t_{IO^8} while leaving t_{IO^2} *unchanged*.[26] Comparing Figs. 8(b) and 8(c) we thus expect that O^8 will occur at smaller κ values and, as κ is increased, the O^2 portion of the phase diagram will grow while that of O^8 will decrease.

Turning to experiment, it has been generally reported,[1–3] as noted schematically in Fig. 1, that BPII occurs at a higher temperature than BPI. However, these results must be interpreted cautiously as in these experiments κ was varied by mixing structurally very different liquid crystal systems. In effect, *all* the parameters in the Landau free energy (1) were varied simultaneously and not just the chirality, as we would desire for comparison with theoretical results. The only exception is the recent study of a chiral-racemic mixture by Marcus and Goodby.[7(d)] By changing relative concentration, these authors succeeded in varying essentially *only* the chirality parameter κ. Thus their results are well suited for comparison with the theoretical phase diagram.

Marcus and Goodby[7(d)] found that as κ is increased BPI only appears between the I and C phases. Its width increases gradually to 0.2 K. At somewhat higher κ, there is a region in which a BPII phase of average width 0.1 K appears between I and BPI. The latter's width in this chirality range is 0.2 to 0.4 K. This region is most similar to other reported phase diagrams.[1–3] Finally, as κ is further increased, BPI disappears and the BPII segment widens sharply to approximate 0.6 K. The first[26] and third chirality regions (i.e., BPI only, BPII only) are in qualitative agreement with the theoretical results discussed above if we identify BPI with O^8 (bcc) and BPII with O^2 (sc). The situation in the intermediate chirality region (BPII followed by BPI as the temperature is reduced) is much more delicate. In fact, higher-order terms[12(f)] in the free energy, which were not included in (1), could be required in order to completely model the experimental results in full detail.

Our assignment of BPI to a bcc space group on the basis of the observed phase diagram is consistent with all the other experimental evidence. Flack and Crooker[3(b)] have identified four polarized Bragg reflections in BPI at wavelength ratios of $1:\sqrt{2}:\sqrt{3}:2$. This would rule out *any* sc group assignment for BPI since the third Bragg ($\langle 111 \rangle$) reflection is polarization independent for all sc structures (see Table IV). The situation for BPII seemed to be more complex. Flack and Crooker[3(b)] (see also Her *et al.*[10]) interpreted their results in terms of *two* distinct phases, BPII*A* and BPII*B*, occurring at larger and smaller κ values, respectively. From the polarized Bragg measurements, BPII*B* was identified[3(b),3(d)] as being bcc while BPII*A*, where only the first two reflections were found, could still be either bcc or sc. This puzzling situation has been considered by Marcus,[7(e)] who has argued convincingly that BPII*B* is not a distinct thermodynamic phase but rather a two-phase, I plus BPI, region. Its occurrence is thus an artifact of the use of mixtures of structurally distinct liquid crystals. BPII*A*, on the other hand, *is* a distinct thermodynamic phase and corresponds to the BPII phase found in the chiral-racemic mixture. This reinterpretation of the BPII*B* data fits in well with our assignment of BPI to bcc O^8 and our argument that the I to BPI transition should occur at lower κ values than the I to BPII one.

The morphological studies of Onusseit and Stegemeyer[11] and Marcus[7(b)] also support our theoretical picture. They have reported that under controlled conditions the BPII phase grows in the form of square platelets. Analysis[7(b)] shows that this is associated with a fourfold (1,0,0) symmetry axis normal to the plane of the platelets. At the BPII to BPI transition, crosshatching is observed within the platelets, as a consequence of the formation of two equivalent sets of $\langle 110 \rangle$ planes normal to the observation direction. These results are all consistent with BPII and BPI having sc and bcc structures, respectively. Interestingly, Onsusseit and Stegemeyer[27] do *not* observe square platelets in the so-called BPII*B* region. This supports the argument of Marcus[7(e)] that BPII*B* is a mixed, two-phase region (I plus BPI) and not a distinct thermodynamic phase.

An additional characteristic of BPI and BPII is the so-called[12(c)] "red shift." This refers to the observed shift (to longer wavelength) of the first BP phase Bragg back reflection with respect to that of the *C* phase. Experimentally,[1–3] the red shift has been found to be 10 to 20% in BPII and 25 to 40% in BPI. Theoretically, for O^2 with an order parameter composed of two spatial frequencies only, we find a red shift of 11–12%, in reasonable agreement with the experimental value. Moreover, numerical calculations based upon (62) and (67) show that the theoretical O^2 red shift is, to better than 1%, *constant* in the region $0.6 < \kappa < 1.4$. This again is in agreement with experimental observations.[1–3]

For O^8, on the other hand, the theoretical red shift calculated with a two spatial frequency order parameter is approximately 10%, much less than all experimental values. This strongly indicates that the order parameter composed of [1,1,0;2] and [2,0,0,2] harmonics used in Sec. II B is *not* sufficient to given an accurate description of the O^8 phase and that additional spatial frequencies are needed. The necessity of including higher harmonics (i.e., [2,1,1;2] and [2,0,0;2]) was noted earlier in our discussion of the theoretical phase diagram, and is further supported by the fact that such harmonics have been observed experimentally in BPI.[2,3(a),3(b)]

Another experimentally accessible quantity is the latent heat associated with the various phase transitions. Using high-resolution differential scanning calorimetric measurements, Stegemeyer and Bergmann[1] showed that the latent heat associated with I→BPII is 30 times greater than that of either BPII→BPI or BPI→*C* in cholesteric esters. Theoretically (see Fig. 5), we find that $[\Delta S_{IO^2}/\Delta S_{O^2C}]_{\max} \simeq 4$, which is considerably smaller than the measured ratio. (Since the BP region is extremely narrow, latent heat and entropy ratios are essentially identical.) One possible cause of this discrepancy is our use of Landau (i.e., mean-field) theory, in which fluctuation contributions to the entropy change are neglected. These are likely to be much greater at an I-BP than at a BP-*C* phase transition, since the former is order-disorder in character while the latter is between two ordered phases. Thus comparisons of theoretical latent heat ratios calculated using Landau theory with experimental ratios are not likely to be useful.

A much more promising approach is to compare calculated and measured order parameter component intensity ratios. Experimentally, these can be determined by measuring the areas under Bragg peaks and noting that the observed optical reflection intensity $I(\sigma)$ for a polycrystalline specimen is proportional to $\lambda^{-1}\epsilon_m^2(\sigma)$, where λ is the wavelength of a given Bragg backreflection and $\epsilon_m(\sigma)$ is defined in (2a). If only $m=2$ amplitudes need be considered, (5) may be rewritten in the form

$$r = \sqrt{2} \sum_{\sigma} I(\sigma) \Big/ \sum_{\sigma} \sigma^{1/2} I(\sigma) \ . \tag{71}$$

Unfortunately, accurate intensity ratios for the observed optical Bragg peaks are not yet available. An estimate can, however, be obtained from the three observed lines (steps) of Meiboom and Sammon.[2] Using (71), we obtain $r = 0.8$, i.e., a red shift of 20%. This is in reasonable agreement with the observed value, $r = 0.73$. Note that since only three lines were measured, the calculated value $r = 0.8$ is in fact an upper bound.

An alternate method of determining relative amplitudes, based upon Darwin width measurements, has been given by Marcus.[7(c)] Based upon his data, we find for the *primary* BP reflections

$$\mu(\mathrm{BPII})/\mu(C) = 0.41 \pm 0.05 \ , \tag{72a}$$

$$\mu(\mathrm{BPI})/\mu(C) = 0.24 \pm 0.05 \ . \tag{72b}$$

Again assigning BPII to O^2 and BPI to O^8, we compare (72a) and (72b) with (68a) and (57a), respectively. In both cases the calculated values are approximately 25% greater than the average experimental ones. The trend, however, is consistent with those structural assignments. Further measurements of this type, particularly for the harmonic amplitudes, will clearly be of great value.

An additional area in which contact with experiment can be made is NMR quadrupolar spectra. Experiments of this type have been reported[4] and show clear differences between BP and C phase spectra. However, no attempt was made to distinguish between BPI and BPII. As pointed out in Secs. II and III, theoretical NMR quadrupolar splittings for polycrystalline systems can be calculated once the order parameter $[\epsilon(\vec{r})]$ is found by minimization of the Landau free energy. The theoretical quadrupolar splitting is obtained by averaging $\sum_{i,j}\epsilon_{ij}\alpha_i\alpha_j$, where α_i are the direction cosines of the applied magnetic field, over a unit cell and over all spatial orientations of the cell with respect to the field. Theoretical NMR quadrupolar spectra for C, O^2, and O^8 structures and a comparison with available experimental data will be given by us elsewhere.

We close by noting that, while we have concentrated our analysis on O^8 and O^2, other structures are also possible. Thus even when it is accepted that BPI is bcc, we see from Table III that the groups T^3 ($I23$) and T^5 ($I2_13$), in addition to O^8, are compatible with the results of Flack and Crooker.[3(b)] While theoretical calculations (see Sec. III B) seem to rule out T^3, the T^5 structure is consistent, both experimentally and theoretically, with the known properties of BPI since T^5 is a subgroup of O^8. Similarly, T^1 ($P23$), a subgroup of O^2, is a possible structure assignment for sc BPII.

In order to distinguish experimentally between the above possibilities, a more complete description of the scattering properties of cholesteric liquid crystal systems is needed. Such a description is provided by the 4×4 Mueller matrix[12(d),28] which relates the polarization state of scattered or reflected light to that of an incident beam at an arbitrary scattering angle. A full analysis of the scattering properties of cholesterics and the Mueller matrix formalism will be given elsewhere. We note here only that initial measurements along these lines have been carried out[3(d)] and that further studies should prove most useful.

Summarizing, we have here presented a detailed analysis of the Landau theory of cholesterics. Extensions of the basic Landau theory to more complex structures have been given. We have emphasized the comparison of model calculations with available experimental data and noted the most promising areas for further theoretical and experimental work.

ACKNOWLEDGMENTS

We are grateful to many colleagues, including particularly S. Alexander, D. Mukamel, and M. Kugler, for useful discussions and comments. We also thank P. P. Crooker, P. H. Keyes, Z. Luz, M. Marcus, S. Meiboom, and H. Stegemeyer for keeping us apprised of their experimental results prior to publication and for helpful clarifications. This work was supported in part by a grant from the U.S.-Israel Binational Science Foundation (BSF), Jerusalem, Israel.

APPENDIX

Using the reduced quantities defined in (9) the average free-energy density (1) becomes

$$f=V^{-1}\int d\vec{r}\,[\tfrac{1}{4}(t\mu_{ij}^2+\xi_R^2\,\mu_{ij,l}^2+\rho\xi_R^2\,\mu_{ij,i}\,\mu_{lj,l}-2\kappa\xi_R^2 e_{ijl}\,\mu_{in}\,\mu_{jn,l})-\sqrt{6}\mu_{ij}\,\mu_{jl}\,\mu_{li}+(\mu_{ij}^2)^2]\;, \tag{A1}$$

with $\rho=c_2/c_1$. To avoid the variational constraint $\mu_{ii}=0$, we add to f the term

$$-V^{-1}\int d\vec{r}\lambda(\vec{r})\mu_{ii}\;, \tag{A2}$$

where $\lambda(\vec{r})$ is a Lagrange multiplier. The extrema of the functional $f[\mu_{ij}]$ are now given by the variational equations

$$\tfrac{1}{2}[t\mu_{ij}-\xi_R^2\,\mu_{ij,ll}-\tfrac{1}{2}\rho\xi_R^2(\mu_{il,jl}+\mu_{jl,il})-\kappa\xi_R^2(e_{iln}\,\mu_{jl,n}+e_{jln}\,\mu_{il,n})]-3\sqrt{6}\mu_{il}\,\mu_{lj}+4(\mu_{ln})^2\mu_{ij}-\lambda\delta_{ij}=0\;. \tag{A3}$$

By setting $i=j$ in (A3) and summing over this index, we obtain

$$\lambda=\sqrt{6}(\mu_{il})^2+\tfrac{1}{6}\rho\xi_R^2\,\mu_{il,il}\ . \qquad \text{(A4)}$$

Substituting (A4) into (A3) gives a set of five independent, coupled, second-order, nonlinear differential equations which, in principle, determine the order parameter μ_{ij}. Since these equations are likely to have more than one solution, one substitutes all μ_{ij} satisfying (A3) and (A4) into (A1) and selects that solution which corresponds to minimal f as the thermodynamic equilibrium state.

---

[1] For a review and references to earlier work, see H. Stegemeyer and K. Bergmann, in *Liquid Crystals of One- and Two-Dimensional Order,* edited by W. Helfrich and G. Heppke (Springer, Berlin, 1980), p. 161.

[2] S. Meiboom and M. Sammon, Phys. Rev. Lett. 44, 882 (1980); Phys. Rev. A 24, 468 (1981).

[3] (a) D. L. Johnson, J. H. Flack, and P. P. Crooker, Phys. Rev. Lett. 45, 641 (1980); (b) J. H. Flack and P. P. Crooker, Phys. Lett. 82A, 247 (1981); (c) Mol. Cryst. Liq. Cryst. 69, 281 (1981); (d) J. H. Flack, P. P. Crooker, and R. C. Svoboda, Phys. Rev. A 26, 723 (1982).

[4] E. T. Samulski and Z. Luz, J. Chem. Phys. 73, 142 (1980).

[5] P. H. Keyes, A. J. Nicastro, and E. M. McKinnon, Mol. Cryst. Liq. Cryst. 67, 59 (1981); A. J. Nicastro and P. H. Keyes, Phys. Rev. A (in press).

[6] D. Armitage and R. J. Cox, Mol. Cryst. Liq. Cryst. Lett. 64, 41 (1980).

[7] (a) M. Marcus, J. Phys. (Paris) 42, 61 (1981); (b) Phys. Rev. A 25, 2272 (1982); (c) 25, 2276 (1982); (d) M. Marcus and J. W. Goodby, Mol. Cryst. Liq. Cryst. Lett. 72, 297 (1982); (e) M. Marcus, *ibid.* 82, 33 (1982).

[8] T. K. Brog and P. J. Collings, Mol. Cryst. Liq. Cryst. 60, 65 (1980).

[9] P. L. Finn and P. J. Cladis, Mol. Cryst. Liq. Cryst. Lett. 72, 107 (1981); Mol. Cryst. Liq. Cryst. 84, 159 (1982).

[10] J. Her, B. B. Rao, and J. T. Ho, Phys. Rev. A 24, 3272 (1981); J. Her and J. T. Ho, in *Liquid Crystals and Ordered Fluids,* edited by A. C. Griffin and J. F. Johnson (Plenum, New York, 1982), Vol. 4.

[11] H. Onusseit and H. Stegemeyer, Z. Naturforsch. 36a, 1083 (1981).

[12] (a) R. M. Hornreich and S. Shtrikman, Bull. Israel Phys. Soc. 25, 46 (1979); (b) J. Phys. (Paris) 41, 335 (1980); Errata 42, 367 (1981); (c) in *Liquid Crystals of One- and Two-Dimensional Order,* edited by W. Helfrich and G. Heppke (Springer, Berlin, 1980), p. 185; (d) Phys. Lett. 82A, 345 (1981); (e) Phys. Rev. A 24, 635 (1981); (f) Phys. Lett. 84A, 20 (1981); (g) R. M. Hornreich, M. Kugler, and S. Shtrikman, Phys. Rev. Lett. 48, 1404 (1982).

[13] S. Alexander, in *Symmetries and Broken Symmetries in Condensed Matter Physics,* edited by N. Boccara (IDSET, Paris, 1981), p. 141.

[14] W. Kuczynski, K. Bergmann, and H. Stegemeyer, Mol. Cryst. Liq. Cryst. 56, 283 (1980); H. Stegemeyer, Phys. Lett. 79A, 425 (1980).

[15] H. Schröder, in *Liquid Crystals of One- and Two-Dimensional Order,* edited by W. Helfrich and G. Heppke (Springer, Berlin, 1980), p. 196.

[16] (a) H. Kleinert, Phys. Lett. 81A, 141 (1981); (b) H. Kleinert and K. Maki, Fortschr. Phys. 29, 219 (1981).

[17] S. Meiboom, J. P. Sethna, P. W. Anderson, and W. F. Brinkman, Phys. Rev. Lett. 46, 1216 (1981); S. Meiboom, M. Sammon, and W. F. Brinkman, Phys. Rev. A (in press); M. Sammon, Mol. Cryst. Liq. Cryst. (in press).

[18] L. D. Landau and E. M. Lifshitz, *Statistical Physics* (Pergamon, Oxford, 1980), 3rd ed., Chap. 14.

[19] P. G. de Gennes, Mol. Cryst. Liq. Cryst. 12, 193 (1971).

[20] S. A. Brazovskii and S. G. Dmitriev, Zh. Eksp. Teor. Fiz. 69, 979 (1975) [Sov. Phys.—JETP 42, 497 (1976)]; S. A. Brazovskii and V. M. Filev, *ibid.* 75, 1140 (1978) [*ibid.* 48, 573 (1978)].

[21] L. D. Landau, Phys. Z. Sowjetunion 11, 26, 545 (1937); *The Collected Papers of L. D. Landau,* edited by D. ter Haar (Gordon and Breach-Pergamon, New York, 1965), p. 193.

[22] Other systems in which a cubic invariant in the free energy can play an important role in determining crystal structures have been discussed by G. Baym, H. A. Bethe, and C. J. Pethick, Nucl. Phys. A175, 225 (1971); S. Alexander and J. McTague, Phys. Rev. Lett. 41, 702 (1978); S. Alexander, R. M. Hornreich, and S. Shtrikman, in *Symmetries and Broken Symmetries in Condensed Matter Physics,* edited by N. Boccara (IDSET, Paris, 1981), p. 379.

[23] *International Tables for X-Ray Crystallography* (Kynoch Press, Birmingham, 1965), Vol. I.

[24] C. C. Yang, Phys. Rev. Lett. 28, 955 (1972).

[25] Y. Poggi, P. Atten, and J. C. Filippini, Mol. Cryst. Liq. Cryst. 37, 1 (1976).

[26] Preliminary calculations by us support this picture.

[27] H. Stegemeyer (private communication).

[28] See, e.g., R. C. Thompson, J. R. Bottiger, and E. S. Fry, Appl. Opt. 19, 1323 (1980).